INVESTIGATING CULTURE CONDITIONS OF *IN VITRO* CARTILAGE MATURATION

by

Abrie Girgis

Thesis submitted in partial fulfillment of the requirements for the degree of

Master of Applied Science in Biomedical Engineering

Department of Chemical and Biological Engineering

Faculty of Engineering

University of Ottawa

ABSTRACT

Articular cartilage (AC) provides an interface between bones within joints that serves to minimize friction, absorb and distribute load along the joint, and facilitate movement. Cartilage has poor self-repair abilities following injury, in part due to the limited migration of chondrocytes and the avascular nature of the tissue which impedes the ability of progenitor cells to reach the site of injury. As a result, cartilage defects are at risk of progressing into osteoarthritis (OA), a degenerative disease of the whole joint. OA affects almost 5 million Canadians and can cause pain, severely reduce joint mobility, and negatively impact quality of life. Cartilage tissue engineering is a field that aims to develop strategies to repair cartilage defects with a combination of cells, biomaterials, and/or cues, either biochemical or biophysical in nature, to guide tissue formation. Tissue engineering strategies can include an *in vitro* maturation phase to create cartilage constructs with sufficient mechanical properties to withstand the cyclic loads present in the joint upon implantation. Identifying optimal culture conditions during this *in vitro* maturation phase is key for the generation of functional cartilage constructs. Typical tissue engineering strategies use supraphysiological glucose concentrations to ensure there is sufficient glucose in the media for energy production and proteoglycan synthesis between media changes; however, studies have found that these elevated glucose concentrations may elicit catabolic processes in the chondrocytes. We hypothesized that culturing constructs at physiological glucose concentrations in larger media volumes, to prevent glucose depletion, would generate cartilage constructs with superior biochemical properties. To test this hypothesis, primary chondrocytes were cultured in physiological (5 mM) and supraphysiologic (25 mM) glucose concentrations at low (2 mL) and high (11 mL) media volumes. The composition of the tissue and the different metabolic pathways conducted by chondrocytes were then evaluated. Our results indicated that high media volumes

generate constructs with significantly higher proteoglycan and collagen content, the two major components of the extracellular matrix. Physiological glucose concentrations had no apparent effect on matrix accumulation; however, histological sections suggest that this culture condition may provide improved cell morphology. The glucose consumption rate was comparable for all four media conditions which suggests that the constructs may have similar matrix synthesis rates. Lactate concentration was significantly higher in low media volumes which may lead to a more acidic environment. The levels of both bioenergetic molecules quantified in the constructs, adenosine triphosphate (ATP) and inorganic polyphosphate (polyP), follow similar trends as the levels of matrix components; however, the relationship between ATP and polyP remains poorly understood. This thesis provides insight into the optimal culture conditions for engineered cartilage by demonstrating that media volume is an important culture parameter for matrix accumulation. Future work is required to understand the mechanisms behind this effect of media volume, to characterize effects of glucose concentration at the cellular level, and to identify key nutrients that will form functional cartilage constructs.

RÉSUMÉ

Le cartilage articulaire fournit une interface entre les os dans les articulations qui sert à minimiser la friction, à absorber et à répartir la charge le long de l'articulation et à faciliter le mouvement. Le cartilage a une faible capacité d'autoréparation après une blessure, en partie en raison de la migration limitée des chondrocytes et de la nature avasculaire du tissu qui empêche les cellules progénitrices d'atteindre le site de la blessure. En conséquence, les défauts du cartilage risquent de progresser en l'arthrose, une maladie dégénérative de l'ensemble des tissues de l'articulation. L'arthrose touche près de 5 millions de Canadiens et peut causer de la douleur, réduire considérablement la mobilité articulaire et avoir un impact négatif sur la qualité de vie. L'ingénierie tissulaire du cartilage est un domaine qui vise à développer des stratégies pour réparer les blessures du cartilage par la combinaison de cellules, de biomatériaux et/ou de signaux, de nature biochimique ou biophysique, pour guider la formation des tissus. Les stratégies d'ingénierie tissulaire peuvent inclure une phase de maturation in vitro pour s'assurer de la formation de tissues avec des propriétés mécaniques suffisantes pour résister aux charges cycliques présentes dans l'articulation. L'identification des conditions de culture optimales pour cette phase de maturation in vitro est essentielle pour la génération de cartilages fonctionnels. Les stratégies de culture typiques utilisent des concentrations de glucose supraphysiologiques pour s'assurer qu'il y a suffisamment de glucose dans le milieu pour subvenir aux besoins énergétiques des cellules et assurer la synthèse des protéoglycanes. Cependant, des études ont montré que ces concentrations élevées de glucose peuvent déclencher des processus cataboliques dans les chondrocytes. Nous avons donc émis l'hypothèse que la culture en présence d'une concentration physiologique de glucose dans des volumes de médias plus importants, pour prévenir l'épuisement du glucose, générerait du cartilage avec des propriétés biochimiques supérieures. Pour tester cette hypothèse,

des chondrocytes primaires ont été cultivés dans des concentrations de glucose physiologiques (5 mM) et supraphysiologiques (25 mM) à des volumes de milieu faibles (2 ml) et élevés (11 ml). La composition du tissu et les différentes voies métaboliques conduites par les chondrocytes ont ensuite été évaluées. Nos résultats indiquent que des volumes élevés de médias permettent la formation de tissus avec une teneur en protéoglycane et en collagène, les deux principaux composants de la matrice extracellulaire du cartilage, significativement plus élevée. Les concentrations physiologiques de glucose n'ont eu aucun effet apparent sur l'accumulation de matrice. Cependant, les coupes histologiques suggèrent que cette condition de culture peut fournir une morphologie cellulaire améliorée. Le taux de consommation de glucose était comparable pour les quatre conditions, ce qui suggère que les tissues peuvent avoir des taux de synthèse de matrice similaires. La concentration de lactate était significativement plus élevée dans les faibles volumes de milieu, ce qui peut produire à un environnement plus acide. Les niveaux des deux molécules bioénergétiques quantifiés dans les tissues, l'adénosine triphosphate (ATP) et le polyphosphate inorganique (polyP), suivent des tendances similaires à celles des composants de la matrice. Cependant, la relation entre l'ATP et le polyP reste mal comprise. Cette thèse donne des pistes sur l’identification des conditions de culture optimales pour le cartilage en démontrant que le volume du milieu est un paramètre de culture important pour l'accumulation de matrice. Des travaux additionels sont nécessaires pour comprendre les mécanismes à l'origine de cet effet du volume des médias, pour caractériser les effets de la concentration de glucose au niveau cellulaire et pour identifier les nutriments clés qui formeront des constructions fonctionnelles du cartilage.

ACKNOWLEDGEMENTS

I would firstly like to thank my supervisor Dr. Jean-Philippe St-Pierre for his continuous support and guidance throughout this project and for giving me the opportunity to experience the excitement research and discovery has to offer.

I would also like to thank my laboratory colleagues, Jordan Nhan, Luisa Metzler, Sietske Barnes, Michael Mulholland, and Noor Ghadie for their help in my research and the fun memories we shared inside and outside the laboratory. I wish to thank Dr. Xudong Cao and his students for their support and for sharing their laboratory space and equipment. Special thanks to Dr. Andrea Serio and all of the members of his laboratory in London (UK) for accepting me as a visiting student for two months and teaching me innovative techniques that I was able to bring back to Ottawa. I am especially grateful for my family for their love and support during the good and challenging times over the past two years.

TABLE OF CONTENTS

LIST OF FIGURES

LIST OF ABBREVIATIONS

AC	Articular cartilage
ACI	Autologous chondrocyte implantation
AGE	Advanced glycation end products
ALP	Alkaline phosphatase
ANOVA	Analysis of variance
ATP	Adenosine triphosphate
BSA	Bovine serum albumin
DAPI	4’,6-diamidino-2-phenylindole
DMEM	Dulbecco’s modified Eagle medium
DMMB	Dimethylmethylene blue
DMOAD	No disease modifying OA drugs
DNA	Deoxyribose nucleic acid
DTT	Dithiothreitol
ECM	Extracellular Matrix
EDTA	Ethylenediaminetetraacetic acid
FBS	Fetal bovine serum
FGF	Fibroblast growth factor
GAG	Glycosaminoglycan
diH_2O	Deionized water
H_2SO_4	Sulfuric acid

HA	Hyaluronic acid
HCl	Hydrochloric acid
HG	High glucose
HK	Hexokinase
HV	High volume
IGF	Insulin-like growth factor
IL	Interleukin
ITS	Insulin-transferrin-selenium
LG	Low glucose
LV	Low volume
MACI	Matrix-assisted ACI
MMP	Matrix metalloproteinase
MPa	Mega Pascale
MTT	3-(4,5-dimethylthiazol-2-yl)-2,5-diphenyl tetrazolium bromide
NAD	Nicotinamide adenine dinucleotide
NADH	Nicotinamide adenine dinucleotide hydride
NMR	Nuclear magnetic resonance
NSAID	Nonsteroidal anti-inflammatory drugs
OA	Osteoarthritis
OH	Hydroxide
PBS	Phosphate buffered saline

PCM	Pericellular matrix
PDMS	Polydimethylsiloxane
PG	Proteoglycan
RNA	Ribonucleic acid
SD	Standard deviation
SO_4	Sulfate
TCA	Tricarboxylic acid
TCTF	Total corrected tissue fluorescence
TGF	Transforming growth factor
TNF	Tumor necrosis factor
UK	United Kingdom
UV	Ultraviolet

INTRODUCTION AND RESEARCH OBJECTIVES

1.1 Introduction

Osteoarthritis (OA) is the most common joint disease affecting nearly 5 million Canadians [1] and the prevalence of OA is expected to continue to increase in part because of the aging population. Those living with OA suffer from pain and reduced joint mobility. The impaired physical function can be detrimental to one's social, mental, and financial well-being. At the morphological level, this disease is characterized by damage to the tissues within the joint including cartilage, bone, ligaments, and synovium [2]. The most recognized characteristic of OA is the progressive degeneration of articular cartilage (AC).

AC is a load bearing connective tissue located on the articulating surface of bones. Its primary functions are to provide a lubricated interface between bones to enable smooth and near-frictionless movement, as well as to transmit and distribute loads across the joint [2], [3]. Cartilage is composed of a dense extracellular matrix (ECM) which consists of water, collagen, proteoglycans, and other biomolecules. The ECM provides cartilage with its mechanical properties and the ability to withstand cyclic load on the joint. Chondrocytes are the only residing cells in cartilage and are responsible for maintaining the ECM components [4]. Cartilage has been shown to have a limited ability to self-repair, owing to a host of factors including its avascular nature, which limits access to injury sites for bone marrow progenitor cells and precludes the formation of a clot in the defect to act as a scaffold for tissue repair [5]. Therefore, cartilage lesions can lead to the progression of joint diseases, including OA, which highlights the importance of developing treatments that repair these lesions [6], [7].

Currently, no disease modifying OA drugs (DMOAD) exist that are capable of curing OA. The majority of treatments available target the related symptoms associated with OA, but do not

halt the progression of the disease. Conservative therapies include lifestyle changes to achieve weight loss and physical therapy to strengthen muscles surrounding the joint [8]. Surgical therapies include cell-based cartilage repair interventions such as marrow stimulation, autologous chondrocyte implantation, tissue replacement by osteochondral auto- and allografts, and advanced OA may require total joint replacement with permanent implants [9]. The cell-based treatment options often yield cartilage with inferior mechanical properties to native cartilage, which emphasizes the need to develop alternative treatments that prevent the progression of this debilitating joint disease and delay or preclude the need for total joint replacements.

Cartilage tissue engineering is an emerging field that aims to repair and regenerate cartilage tissue by providing cells with chondrogenic potential with an instructive micro-environment to guide tissue formation through carefully designed scaffolds and/or the presentation of biomolecular and biophysical signals [10]. It is crucial that these engineered cartilage constructs can withstand the cyclic loading of the joint throughout the repair process. While this can theoretically be achieved through the design of the scaffold mechanical properties, this is a challenging endeavor and, therefore, many cartilage tissue engineering strategies have relied on *in vitro* incubations of different lengths of time to allow the constructs to mature prior to transplantation into the joint. The project presented in this thesis will focus specifically on this *in vitro* maturation phase since this phase is critical to the functional outcome of the constructs. A broad range of strategies have been explored to mimic physiologic conditions with *in vitro* culture, including culturing cells with growth factors that stimulate anabolic processes, applying physiologic deformational loading that native AC experiences, and culturing cells in a low-oxygen environment [11]–[16]. Although significant progress has been made in cartilage tissue

engineering and identifying beneficial *in vitro* culture conditions, the resulting cartilage constructs do not yet exhibit comparable biomechanical and biochemical properties to native cartilage.

Another factor that governs the functional development of cartilage constructs is the nutrient environment in which they are cultured. It is important to identify key nutrients within the culture medium and then monitor and replenish them as needed, either through traditional media changes or via the design of more complex continuous flow bioreactors. Glucose is one key nutrient for mammalian cell culture since it is the substrate for glycolysis, the main mechanism for ATP production [17]. In cartilage, glucose also acts as a building block for proteoglycan synthesis [18]. At high cell seeding densities, the nutrients tend to deplete quickly as they are consumed, and waste products accumulate which can be detrimental for cell phenotype and viability. As a result, high glucose concentrations are often used for culturing cartilage constructs in order to meet the metabolic demands of chondrocytes and synthesize essential ECM components [19]. However, high glucose concentrations can be harmful to the integrity of the tissue and has been shown to induce nonresponsiveness to anabolic growth factors, such as IGF, and stimulate chondrocyte catabolic processes [20], [21]. In contrast, culturing constructs in larger media volumes is conducive to overcoming a limited nutrient supply and has demonstrated improved cartilage tissue growth, but is also associated with higher costs [19], [22].

For this project we are interested in culturing cartilage constructs at glucose levels that are representative of normal physiological conditions. In order to overcome the potential of depleting nutrients, we also tested the effects of increasing the volume of culture media to maintain a stable nutrient environment. We are also interested in characterizing the production of bioenergetic molecules by chondrocytes under the different culture conditions. The consumption of glucose, production of ATP, and release of lactate are all parameters of interest. Another intriguing

biomolecule involved in chondrocyte metabolism is inorganic polyphosphate (polyP). PolyP is a linear polymer of orthophosphate residues linked by high energy phosphoanhydride bonds that are also present in ATP [23]. PolyP resides in every living cell in nature and has various functions depending on the organism, type of cell, and subcellular compartment it is located in [24]. Despite its ubiquity, its functions are not fully understood in mammalian tissues. This is in part because the quantity of polyP is much smaller in mammals than microorganisms, including yeast and bacteria, which makes the transfer of quantification methods particularly challenging [25]. Previous work has shown that exogenously administered polyP stimulates the accumulation of cartilage ECM components such as glycosaminoglycans (GAG) and collagen within *in vitro*-formed cartilage [26]. We are interested in monitoring the endogenous levels of polyP in the cartilage constructs as part of our efforts to gain an understanding of how it interacts with chondrocytes. This new knowledge can promote the development of biomaterials that exploit this biomolecule for cartilage tissue engineering.

1.2 Hypothesis and Research Objectives

Here, we **hypothesize** that culturing cartilage constructs at physiological glucose concentrations and in high media volume to provide a more stable nutrient environment throughout the culture period, will yield *in vitro*-formed cartilage constructs with superior biochemical and biomechanical properties compared to the high glucose media typically used for high cellularity tissue engineering cultures.

To test this hypothesis, primary chondrocytes will be cultured at high density to form 3D tissues at physiological (5 mM) or high (25 mM) glucose levels and in low (2 mL) or high (11 mL) media volumes over a period of 4 weeks. This project has two main research objectives that will contribute to testing our hypothesis:

1. Characterize the composition and mechanical properties of *in vitro*-formed cartilage constructs cultured with different glucose concentrations and media volumes.
2. Investigate the different metabolic pathways conducted by chondrocytes within *in vitro*-formed cartilage constructs cultured with different glucose concentrations and media volumes.

LITERATURE REVIEW

2.1 Articular Cartilage

2.1.1 Functions of AC

AC is a thin layer of soft connective tissue located on the articulating surface of bone in diarthrodial joints, including the shoulder, elbow, hip, and knee. It is aneural, alymphatic, and avascular under normal physiologic conditions. AC is subject to a harsh biomechanical environment and is able to withstand high cyclic complex loading while enabling movement and mobility. The principal functions of AC are to provide a low friction surface and to absorb and distribute load along the joint.

2.1.2 Composition of AC

The complex composition of AC gives rise to the function of this specialized connective tissue. AC is commonly referred to as a biphasic model that constitutes a solid phase and a fluid phase. The solid phase of AC is comprised of chondrocytes, the residing cells in cartilage that occupy 1-5% of the total volume depending on age and location in the joint, as well as an extracellular matrix (ECM) which occupies most of the tissue and is composed of proteoglycans, collagens, and non-collagenous proteins [27]. The fluid phase of AC constitutes the interstitial fluid that moves throughout the matrix [28]. These elements work together to provide AC with its mechanical properties in order to perform its necessary functions within the joint.

2.1.2.1 Chondrocytes

Chondrocytes are the only residing cells in AC. These highly specialized cells are responsible for maintaining tissue homeostasis by regulating the breakdown, synthesis, assembly and organization of ECM components [29]. Each cell is surrounded by a dense pericellular matrix (PCM) that

entraps the chondrocyte and prevents migration into adjacent regions of cartilage. A chondrocyte and its surrounding PCM together form an entity known as the chondron and represent the primary functional unit of the tissue [29], [30]. The number, size, and shape of chondrocytes vary depending on their anatomical region and depth within cartilage tissue. Chondrocytes at the superficial zone are small, flat, and present at a high cell density compared to those in deeper regions of the tissue which are large, round, and present at a low cell density [31]. Chondrocytes have low proliferative activity which contributes to the limited capacity to repair cartilage in response to injury [32]. An optimal chemical and mechanical environment is critical for the survival of chondrocytes and maintenance of tissue homeostasis.

2.1.2.2 Proteoglycans

Proteoglycans (PG) consist of a protein core with glycosaminoglycans (GAG) covalently bound to form a bottlebrush-like structure, representing about 10% of the tissue dry weight [33]. PGs have a high degree of diversity due to the different cores and different nature and numbers of GAGs, which contributes to their involvement in multiple biological processes [34]. GAG side chains are long unbranched polysaccharide molecules containing repeating disaccharide units. In cartilage, the most common GAGs are dermatan sulfate, keratan sulfate, chondroitin 4-sulfate, chondroitin 6-sulfate, and hyaluronic acid (HA). HA is the only GAG that does not contain negatively charged sulfate groups and forms non-covalently linked complexes with PGs to produce aggregates of PG, as illustrated in Figure 1. PGs are important structural components of AC that hydrate, protect, and lubricate the tissue [34].

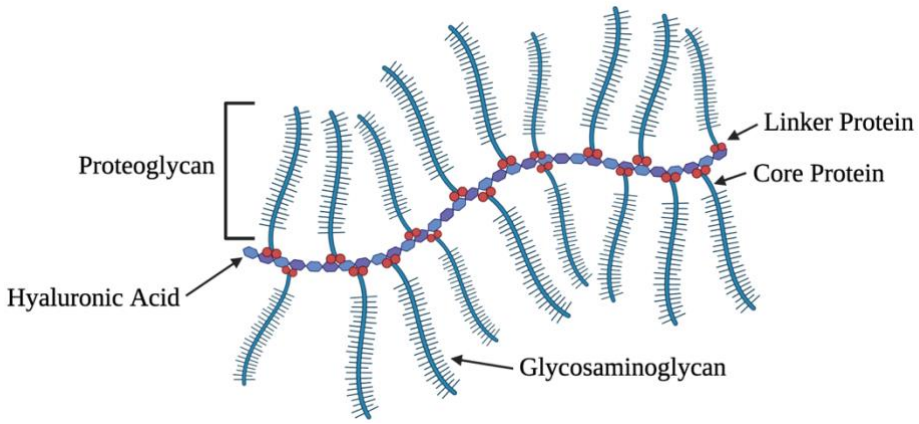

Figure 1. Schematic representation of an aggregate of PG found in the ECM of cartilage.

2.1.2.3 Collagens

The most abundant macromolecule in ECM is collagens which accounts for about 60% of the dry weight of cartilage tissue [35]. Collagens are structural proteins composed of three polypeptide chains that self-assemble into a triple helix. Each chain consists of three repeating amino acids where every third amino acid is glycine, resulting in a Gly-X-Y sequence. The amino acids that occupy the X and Y positions are often proline and hydroxyproline, respectively. The triple helical procollagen molecules are cleaved at the amino and carboxy termini by specific proteases prior to self-assembling into collagen fibrils which are further organized into collagen fibers [36]. These fibers are organized into complex collagen networks by processes that have yet to be fully elucidated.

Collagen type II is the most predominant collagen found in AC, with other collagens including type III, VI, IX, X, XI, XII, and XIV present in relatively smaller amounts [37]. Collagen type II is a homotrimer composed of three identical α_1(II) chains that form the backbone of collagen fibrils [36]. Collagen type IX is cross-linked to the surface of collagen fibrils in an antiparallel fashion and may be involved in the cross-linking of the interfibrillar network [31]. Collagen type XI is present within and on the surface of collagen fibrils, where it initiates fibril self-assembly and

regulates fibril size [31]. Collagen type VI is located in the PCM and is involved in the mechanotransduction of the tissue [38]. Collagen type X is found in the deep zone of cartilage and may play a role in the calcification of cartilage [39].

2.1.2.4 Fluid Phase

The fluid phase contributes up to 80% of the wet weight of AC and plays a large role in the ability to withstand significant loads [27]. The fluid phase contains small metabolites including sodium, calcium, chloride, and potassium [29]. Some of the water can move freely in and out of the matrix at the articular surface which influences the compressive stiffness of the tissue. The fluid phase acts as a medium to transport and distribute nutrients to chondrocytes and provides lubrication for the tissue.

2.1.3 Mechanical Properties of Cartilage Tissue

The biphasic viscoelastic nature of AC confers its mechanical behaviour in response to compression loading. In the presence of load, the hydrostatic pressure increases because of the relative incompressibility of water. The interstitial fluid subsequently flows out of the tissue which generates frictional drag on the tissue and transmits load along the joint [3]. When cartilage is compressed, the negatively charged aggregated proteoglycans are pressed closer together which in turn creates stronger repulsion and expansion against the collagen framework [28]. When a constant load is applied, the tissue will exhibit a stress-relaxation process characterized by a peak stress level, followed by deformation in a time-dependent manner until an equilibrium is reached. Rehydration of the tissue after load is removed is achieved through the Donnan effect, whereby the negatively charged proteoglycans attract cations from the fluid phase which increases osmolarity and fluid flow through the tissue [3], [40].

AC relies on the extensive collagen fibrillar network for its mechanical strength [41]. The collagen network resists the expansion of the ECM from the high osmotic pressure and opposes the tensile and shear forces encountered during articulation [42]. Once the network is fully developed, there is limited ability for chondrocytes to regenerate collagen after degeneration or mechanical injury because of relatively low synthesis rates.

2.1.4 Organization of ECM

AC is organized in a highly ordered structure that reflects its functions. Morphological changes of the tissue occur with respect to the depth from the articulating surface and the distance from the chondrocytes. The different zones can be characterized by changes in the composition, organization, and function of the matrix. Figure 2 illustrates the complex structure of articular cartilage and the different zones and regions will be discussed in further detail.

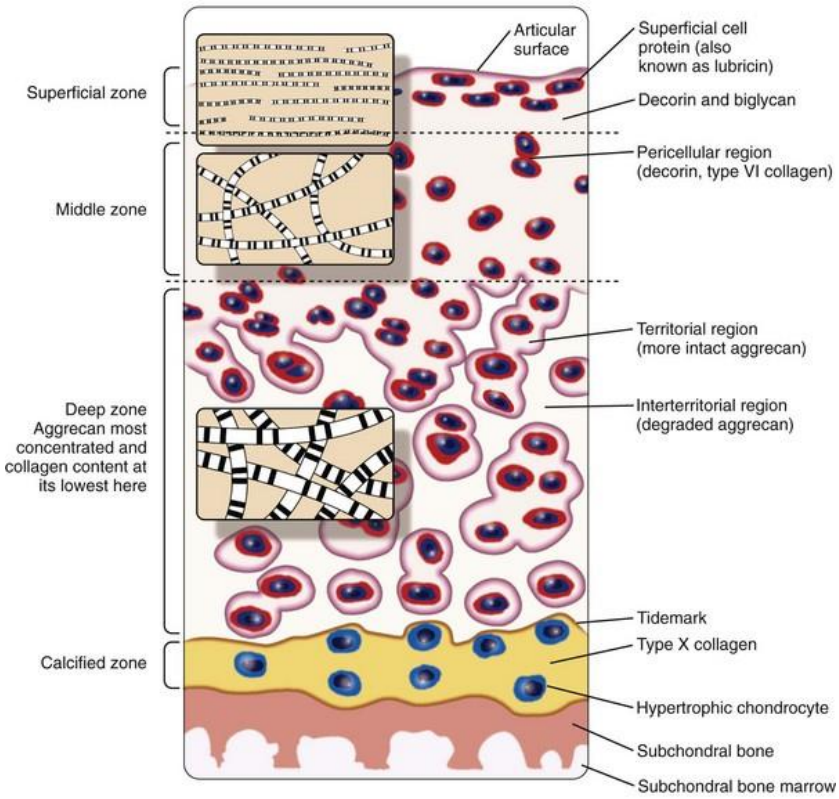

Figure 2. Schematic representation of the different zones and regions of articular cartilage. (Reprinted with permission from the Composition and Structure of Articular Cartilage: A Template for Tissue Repair [31])

2.1.4.1 Zonal Organization

AC is typically reported as being organized into four zones from the articular surface to the subchondral bone, namely the superficial zone, middle or transitional zone, deep zone, and the zone of calcified cartilage. Each zone differs with respect to the content of water, PGs, and collagen, and the size of the aggregates, as well as their organization. The morphology of chondrocytes, their phenotype, and their metabolic activity also differ between each zone.

The superficial zone is at the articular surface and is in contact with synovial fluid. This zone consists of a dense sheet of collagen fibrils oriented parallel to the articular surface. Beneath

the collagen fibrils are flattened ellipsoid-shaped chondrocytes located in a matrix with high collagen concentrations and low PG concentrations compared to other zones. The concentration of water is also highest in the superficial zone. The matrix of collagen fibrils provides this zone with greater tensile stiffness and strength compared to other zones which enable it to withstand shear and tensile forces caused by articulation. This layer also limits the movement of molecules in and out of the tissue due to the dense collagen meshwork at the surface of AC and its integrity is critical for the protection and maintenance of deeper layers.

The middle zone is immediately deep to the superficial zone and is composed of thicker collagen fibrils that are oriented randomly. The chondrocytes are spherically shaped at low cell density and demonstrate more metabolic activity compared to the superficial zone. This layer is rich in PG content which enables it to absorb and resist compressive forces in the joint.

The deep zone contains the thickest collagen fibrils that are oriented perpendicular to the joint surface. Collagen and water content are the lowest in this zone, meanwhile PG content is the highest compared to other zones. Large spherical chondrocytes occupy this zone and are oriented in columns. Functionally, the deep zone provides the greatest resistance to compressive forces during articulation [29].

The zone of calcified cartilage is a thin mineralized region of the deep zone that anchors hyaline cartilage to the subchondral bone. Because of its intermediate stiffness compared to the soft cartilage and much stiffer subchondral bone, it is thought to ensure the mechanical integrity of the interface. The calcified zone is separated from the deep zone by the tidemark where collagen fibrils are oriented perpendicular and bridge the two zones. Chondrocytes in this zone have a hypertrophic phenotype and can synthesize collagen type X and calcify the ECM [31].

2.1.4.2 Regional

Three different regions dependent on the proximity to the chondrocytes exist: the pericellular matrix, the territorial matrix, and the interterritorial matrix. The pericellular matrix immediately surrounds the chondrocyte and is rich in PG content and collagen type VI [43]. The pericellular matrix mediates communication between the ECM and the chondrocyte and manages matrix turnover [43], [44]. The territorial matrix surrounds the pericellular matrix and is composed of thin collagen fibrils. The interterritorial matrix is characterized by large collagen fibrils and constitutes the majority of the tissue. This region contributes most to the biomechanical properties of AC [29].

2.2 Osteoarthritis

Osteoarthritis (OA) is the most common joint disease in the world, affecting 10% of men and 18% of women over the age of 60 [45]. Although it is primarily recognized by a loss of cartilage, OA is a degenerative disease of the entire joint. It involves changes in multiple tissues within the joint including the degeneration of AC, formation of bone spurs, changes in the subchondral bone, and inflammation of the synovium. This musculoskeletal disease is a source of pain, stiffness, and dysfunction of the joint that results in limited movement and substantially reduced quality of life.

2.2.1 Etiology

OA is a multifactorial disease where both systemic factors and biomechanical factors play a role in determining the risk of developing OA. Systemic factors may increase the susceptibility of joints to injury and include age, gender, sex hormones, bone density and osteoporosis, race, nutrition, and genetics [46]. Local biomechanical factors act on individual joints and determine the ability to distribute load across the joint. These factors include obesity, acute injury and repeated joint loading, joint deformity, and muscle strength [46].

At the molecular level in cartilage, chondrocytes fail to maintain homeostasis between the synthesis and degradation of the ECM components. During the progression of OA, chondrocytes express pro-inflammatory cytokines including IL-1β, TNF-α, IL-6, and IL-17 [47]. These catabolic mediators increase the level of matrix-degrading enzymes and reduce the synthesis of ECM proteins [48]. In response, chondrocytes increase synthesis of matrix components and proliferate which can lead to a temporary increase in cartilage thickness. Despite these initial efforts to maintain the integrity of the tissue, they do not compensate for the loss of ECM and the catabolic mechanisms take over [47], [49]. The loss of homeostasis leads to a reduction in PG content and weakening of the collagen network, thereby impeding the mechanical properties of the tissue [49], [50]. It is not yet known what initiates these imbalances, however, it is most likely a combination of the risk factors mentioned above that leads to cartilage damage. It is also likely that the factors involved differ between individuals.

Cartilage defects are injuries or damage to the tissue that can vary in size and depth, where partial thickness defects are confined within the AC layer whereas full thickness defects penetrate the subchondral bone. Partial thickness defects have poor healing potential partly because chondrocytes are entrapped within their chondron and cannot migrate to the site of injury, as well the avascular nature of the tissue limits access to progenitor cells and the formation of a fibrin clot that can act as a scaffold for the repair process [5]. Conversely, when a full thickness defect occurs, blood from the marrow fills the injury site and forms a clot containing inflammatory cells. Mesenchymal progenitor cells subsequently reach the defect and differentiate into chondrocytes that generate a repair tissue [5]. This self-healing capacity results in fibrocartilaginous tissue that is inferior to hyaline cartilage and is eventually subject to degenerative changes for many

individuals [5], [7]. If left untreated, these defects can cause degenerative processes that progress into diseases such as OA, which highlights the importance of repairing these lesions.

2.2.2 Treatment Options

Currently, there are no disease modifying OA drugs (DMOAD) available that can stop or revert the progression of OA. A lack of DMOAD's is in part due to an incomplete understanding of the complex and multifactorial pathogenesis of the disease, the discordance between symptom and structure, the inability to detect early stages of OA, and the challenges associated with delivering drugs to the joint [51], [52].

Therapeutics clinically available today aim to minimize pain and improve joint function by targeting the symptoms of OA and do not improve the joint structure itself. A number of therapeutic modalities exist and are often used synergistically with other treatment strategies and should be individualized for each patient. Treatments for OA and joint defects with a high probability of progressing to secondary OA can be classified as either conservative therapy or surgical therapy.

2.2.2.1 Conservative Therapy

Conservative therapies are often the first methods used to manage the early stages of OA because they are non-invasive. These treatments include both non-pharmacological and pharmacological modalities that aim to alleviate symptoms associated with OA, but do not exhibit disease-modifying effects. Non-pharmacological methods include lifestyle changes that lead to weight loss, avoiding activities that aggravate the condition, and physical therapy that strengthens the muscle and improves joint mobility [53]. The use of braces and orthoses are also effective at reducing pain and joint stiffness [54]. Pharmacological agents include nonsteroidal anti-inflammatory drugs (NSAIDs) and opioids that exert anti-inflammatory and analgesic effects.

Intra-articular injection is a form of local administration that is offered when orally administered analgesics no longer provide pain relief for the patient. Long-acting corticosteroids can be injected in the joint to relieve pain which lasts between 2-4 weeks [55]. HA derivatives act as a lubricant and can compensate for the deficiency of HA in OA joints [55].

2.2.2.2 Surgical Therapy

When conservative treatments are not effective at relieving the patient from pain, surgical treatments should be considered. Repairing lesions at risk of tissue degeneration reduces the risk of these defects progressing into OA. Surgical interventions aim to repair cartilage lesions either by transplanting healthy cartilage or by stimulating regeneration of the tissue. These strategies include marrow stimulation, autologous chondrocyte implantation (ACI), osteochondral auto- and allo-grafts, and joint replacement.

Marrow stimulation is a cell-based surgical technique that relies on the body's healing capabilities in order to repair cartilage lesions. In this procedure, damaged cartilage is removed by debridement and the underlying subchondral bone is damaged to induce bleeding. The bleeding leads to the formation of a blood clot that is infiltrated by mesenchymal stem cells, which deposit fibrocartilaginous tissue at the damaged site [56]. The marrow can be stimulated via damage to bone using different techniques, including drilling, abrasion, and microfracture, where microfracture is the most common because it is easy to use and avoids heat damage [56]. The fibrocartilaginous tissue that covers the full-thickness lesion is mechanically inferior to the original articular cartilage, however, it does relieve patients of symptoms for several years.

ACI is another cell-based surgical technique that involves a 2-stage procedure to repair lesions. For the first stage, cartilage is harvested from low weight-bearing areas of the joint. The harvest undergoes enzymatic digestion to isolate the chondrocytes, which are then cultured *in vitro*

to increase the number of cells. The second stage of the procedure is reimplantation of chondrocytes into the cartilage lesion. The chondral defect is debrided to remove loose and damaged fragments of tissue, and the chondrocytes are implanted underneath a periosteal patch or collagen membrane sutured over the defect [57]. Following ACI, the cells deposit cartilage-like tissue that remodels over a period up to 3 years until it reaches complete maturation that is characterized by hardening of the tissue and complete integration between tissue graft, native cartilage, and the underlying subchondral bone [58]. Clinical applications of ACI have been successful in relieving patients from pain and improving joint function; however, it is not yet standard practice due to high costs and limited long-term success, and is currently not conducted in Canada. During the *in vitro* chondrocyte expansion process, cells must be cultured in monolayer which leads to dedifferentiation. Dedifferentiated chondrocytes down regulate the expression of type II, IX, XI collagen, and aggrecan resulting in a mechanically inferior ECM that may explain the poor long-term prognosis [59].

Osteochondral grafting is another surgical technique that aims to restore damaged cartilage. This procedure involves the transplantation of healthy cartilage from non-weight bearing areas of the joint to small cartilage defects. This method is technically demanding and is limited by the amount of available graft from the donor site [60]. Osteochondral allografts can be used to repair larger lesions, but face challenges of reduced viability due to storage, immunogenicity, risks of disease transmission, and availability [60].

Previous methods described aim to repair lesions at risk of progressing into secondary OA. For severe cases of OA, total joint replacement is an effective solution to relieve the patient from pain and improve their mobility. Prosthesis made of a combination of materials, including metals, ceramics, and polymers, replace the joint and recreate the articulating function. This procedure is

generally successful in restoring movement and relieving pain in 90% of patients [61]. The long-term outcome of the joint replacement depends on the survival of the prosthesis. Some reasons for implant failure include aseptic loosening, infection, dislocation, and fracture, which influence the need for surgical revision [61]. The invasive nature of the surgeries, the potential complications associated with these implants and their limited lifespan makes total joint replacement an undesirable treatment option for younger patients [62]. Although it is a suitable treatment option for end-stage disease, research and development should prioritize disease prevention and tissue regeneration strategies.

2.3 Cartilage Tissue Engineering

The current cell-based clinical treatment methods mentioned above to repair AC defects have shown success in relieving pain and recovering function for a short time; however, these methods have shown limited long-term outcome for many patients, in part because of the durability of the repair tissue. To overcome the limitations of these cell-based therapies and eventually achieve long-term functional repair or even regeneration of AC defects, the field of cartilage tissue engineering has been developing promising alternatives in which a plethora of cell-based, tissue engineered products have been developed [63]. Matrix-assisted ACI (MACI) is a relatively new version of ACI that applies concepts of tissue engineering by culturing autologous chondrocytes on a scaffold before it is implanted in the defect. Cartilage tissue engineering involves the combination of carefully selected cells with biomaterial scaffolds and biological and/or biophysical signals that provide a microenvironment to guide and stimulate regenerative processes. There have been a large number of studies performed that investigate each of these elements of tissue engineering in the search for optimal strategies and key concepts have been reviewed extensively [10], [11]. Ultimately, identifying a strategy that leads to the generation of cartilage

constructs with biological and mechanical properties comparable to native tissue would offer promising results for long-term cartilage tissue repair.

Because AC fulfills primarily biomechanical functions in the body and is exposed to a high number of elevated cyclical loads over the lifetime of an individual (e.g. an average individual takes approximately one million steps in a year), it is important for engineered cartilage constructs to be designed to withstand these loads immediately upon transplantation. While many efforts have focused on the development of scaffolds with sufficient mechanical properties to withstand the high mechanical demands of the joint, this strategy often requires compromises with other properties of the scaffold. For this reason, many strategies include an *in vitro* tissue maturation period to allow the cells to produce ECM. The success of this *in vitro* maturation phase relies on the determination of optimal culture conditions whereby the microenvironment dictates the functional development of the construct [64], [65]. Several strategies have been investigated to improve the biosynthetic capacity of chondrocytes and stimulate tissue formation. The use of growth factors has demonstrated anabolic properties and include members of the TGF-β superfamily, the FGF family, and IGF-1 [14]. This approach is limited by the ability of these relatively large molecular weight molecules to diffuse within a range of scaffolds and hydrogels. Studies have also shown that mechanical stimulation yields increased matrix accumulation and enhanced mechanical properties of the engineered tissue [19], [66]–[69]. Chondrocytes cultured in low-oxygen tension that mimics the physiological environment of the joint displayed increased proliferation and matrix accumulation compared to atmospheric oxygen levels [13], [70]. Despite significant progress in generating engineered cartilage using these strategies, the biochemical and mechanical properties of the cartilage constructs are not yet comparable to native cartilage. Further

studies are required to deepen our understanding of the conditions that stimulate tissue formation in order to develop high-quality cartilage constructs.

Another key parameter that influences the development of *in vitro* cartilage tissue formation is the culture medium and nutrient environment. Within the joint, chondrocytes rely on the diffusion of nutrients from the synovial fluid for ECM maintenance which has led to multiple investigations into the role of nutrient availability on engineered constructs *in vitro* [19], [71]. Glucose has been identified as a key nutrient in culture medium for cell viability. However, at high cell seeding densities encountered in tissue engineering applications, the nutrient supply depletes quickly and may lead to issues with the mechanical and biochemical properties of the engineered constructs [15]. In traditional batch-fed cultures, constructs are typically cultured in high concentration glucose environments (e.g. 4.5 g/L) to ensure that there is a sufficient amount of nutrients to support the metabolism of the cells. However, increasing glucose concentrations can be harmful to chondrocytes and induce nonresponsiveness to key growth factors, such as IGF-1 [20]. High glucose concentrations have also been associated with increased levels of matrix metalloproteinases (MMPs), the class of enzymes that degrade tissue matrix [21]. For these reasons, culturing chondrocytes in high glucose environments may not be suitable for generating cartilage constructs with sufficient biochemical and biomechanical properties that will survive after implantation.

Media volume is another parameter that influences nutrient availability and can be manipulated as an alternative to raising concentration, where larger media volumes are favorable to maintain high cell density, cell viability, and matrix production [19], [22]. The exact mechanism that explains why higher media volume is more desirable for cartilage constructs is not fully understood, yet several potential mechanisms exist. As eluded to above, glucose may be the

limiting factor as a key nutrient in the media since it is liable to cellular consumption and its depletion in lower media volumes may have detrimental effects on the integrity of the tissue [22]. Smaller media volumes may also be more susceptible to higher concentrations of waste products including lactate, which can have inhibitory effects on matrix accumulation and cell viability [17]. The application of hydrostatic pressure on cartilage constructs has been shown to enhance the biomechanical and biochemical properties of the engineered tissue [12]. Therefore, hydrostatic pressure may play a role in the integrity of the cartilage constructs if the height of the media column changes to accommodate a change in media volume. Changes in vessel dimensions, if they impact the surface area to volume ratio, could impact dissolved oxygen levels and impact chondrocyte metabolism [22]. The field of tissue engineering benefits from investigating the precise mechanism that explains why higher media volumes are superior because it can determine the optimal microenvironments for cartilage constructs and develop a better understanding of chondrocyte metabolism.

2.4 Cartilage Bioenergetics

Due to the avascular nature of AC, chondrocytes access nutrients through diffusion from the synovial fluid and to a lesser extent from the arteries of the subchondral bone. Glucose is a key nutrient critical for chondrocyte metabolism.

Glucose is the substrate for glycolysis which results in a net gain of 2 adenosine triphosphate (ATP) molecules and the production of pyruvate. Pyruvate is either transported into the mitochondria where it is converted to acetyl-CoA and enters the tricarboxylic acid (TCA) cycle, or it is converted to lactate and exits the cell [72]. Based on several lines of evidence, cartilage tissue relies predominantly on glycolysis for ATP production [73]. Compared to other tissues, mitochondrial oxidative phosphorylation has a minor contribution to energy formation in

cartilage. Glucose can also be stored as glycogen to serve as an energy reserve and is a building block for the synthesis of proteoglycans [72]. Changes in the extracellular glucose concentration has a direct impact on some of the functions of chondrocytes. For example, responsiveness to the anabolic growth factor IGF-1 was lost at non-physiological glucose concentrations [20]. Reports have also shown that a depletion as well as an increase in glucose levels promotes catabolic processes of cartilage due to increased expression of MMPs [21], [74]. These studies support a potential increased risk of developing OA in patients with diabetes mellitus. Therefore, the maintenance of steady glucose levels in native cartilage is critical for chondrocyte metabolism and matrix synthesis.

The low demand of oxidative phosphorylation in cartilage promotes the conversion of pyruvate to lactate as the end-product of glycolysis. This conversion regenerates the NAD+ required for ATP production during glycolysis [75]. Due to the pKa of lactate, at physiological pH lactic acid exists predominantly as H+ and lactate- ions which has direct impact on the tissue pH [72]. Changes in the physiochemical environment can impact cartilage integrity. Acidic conditions have been shown to decrease ATP production, cell viability, and inhibit matrix synthesis [76], [77]. In order to maintain intracellular pH, efflux of lactate- and H+ ions is mediated by cotransport proteins called monocarboxylate transporters [73].

Matrix synthesis is dependent on ATP as the currency of energy in the tissue. Reduction in ATP levels can cause a reduction in proteoglycan synthesis [78]. Suppression of glycolysis by anoxia, glycolytic inhibitors, or low pH demonstrated a decrease in intracellular ATP levels which is required for DNA, protein, proteoglycan, and HA synthesis [78], [79]. Maintaining extracellular levels of ATP and adenosine, its metabolite, is also important for tissue homeostasis and prevents phenotypic changes associated with the progression of OA [80]. The levels of glucose as an energy

source, ATP as energy currency, and lactate as a by-product provides insight into the metabolic state of the cell and are investigated in this project. Another metabolite that has not been investigated as thoroughly is inorganic polyphosphate and will be discussed in the following section.

2.5 Inorganic Polyphosphate

Inorganic polyphosphate (polyP) is a linear polymer of orthophosphate residues linked by high energy phosphoanhydride bonds (Figure 3). The chain length of polyP can range from 2 up to several thousand phosphate residues. PolyP has a natural occurrence in all three branches of the phylogenetic tree and is hypothesized to be conserved from prebiotic times, preceding the evolution of RNA, DNA, and proteins [24]. PolyP has several different functional roles depending on which species, cell, and subcellular compartment it is located in, as well as its molecular weight and when it is needed by the organism.

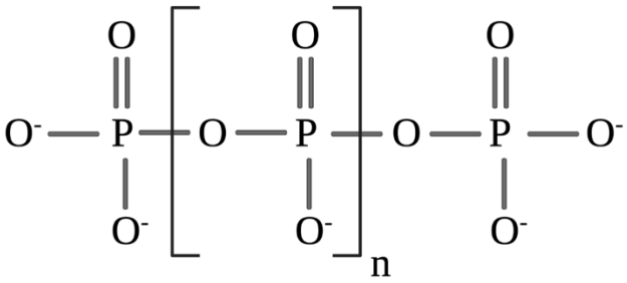

Figure 3. Chemical structure of inorganic polyphosphate.

2.5.1 Biological Roles of polyP

In microorganisms including yeast and bacteria, polyP plays important functions in providing phosphorus and energy stores, in cation homeostasis, in transcription, and in the stress response [81], [82]. There has also been significant progress in understanding the physiological roles of polyP in mammalian cells. PolyP released from platelets acts as a pro-coagulant and pro-

inflammatory mediator [83]. Also, polyP has been identified to modulate ion channel activity and has demonstrated a role in differentiating human mesenchymal stem cells into osteoblastic cells [84], [85].

One of the most intriguing features of this molecule is the possibility that polyP acts as an energy metabolite and is a key component of mammalian bioenergetics. Interestingly, this molecule has relatively high levels localized in the mitochondria, the site of oxidative phosphorylation, and is composed of phosphoanhydride bonds which are also found in ATP [81]. Recently, it has been discovered that the levels of polyP in mammalian mitochondria are highly dynamic and are related to the energetic state of mitochondria [86]. In mammalian tissues, there is a direct link between the production of polyP with mitochondrial respiration and oxidative phosphorylation [86]. Some evidence that supports this link is that polyP production in mitochondria may be conducted through a process that involves the enzyme responsible for ATP production, F0-F1-ATP synthase, and does not require ATP as a substrate [86]. Importantly, polyP can be hydrolyzed by ATP synthase instead of ATP [87]. PolyP was also suspected to be involved in the activation of the mitochondrial permeability transition pore, a structure involved in stress-induced cell death [88]. PolyP plays a key role in the buffering system of free mitochondrial calcium following calcium uptake and enables elevated levels of calcium within the organelle [89]. Calcium homeostasis is critical for the regulation of cellular metabolism and ATP production.

The role of polyP in cartilage tissue is of particular interest for this project. St-Pierre et al. [90] was the first to report that polyP has an anabolic effect on both *in vitro* engineered AC and native AC cultured *ex vivo.* This anabolic effect is the result of polyP promoting the accumulation of GAG and collagen, two major components of the ECM, in a chain length and concentration dependent manner. Interestingly, the DNA content of tissues treated with polyP increased at a

slower rate than the untreated tissues despite having proliferating effects on other cell types, including fibroblasts and mammary cancer cells [91], [92]. PolyP may be exerting chondroprotective mechanisms in these tissues since chondrocyte proliferation is characteristic of cartilage pathologies, including OA [93]. In another study, polyP was injected in the knee joint of guinea pigs which slowed the progression of cartilage degeneration [26]. PolyP treatment has led to increased ATP production and cell proliferation which offers insight into the pro-anabolic effects on matrix formation, yet the mechanism of action remains unknown [94]. For this project, we are interested in deciphering the modulation of endogenous polyP in cartilage tissue cultured in different media conditions.

2.5.2 Characterization of polyP

As touched on above, polyP has received scant attention and its biological functions are only recently being discovered. The major barrier that prevents this biomolecule from being thoroughly investigated is the limited methods available to characterize polyP. The parameters of interest when analyzing polyP include the concentration, chain length, cellular localization, and the cation composition. Levels of polyP in mammalian tissues are quite low compared to those present in prokaryotes which contributes to the challenge of developing sufficiently sensitive methods for characterizing polyP [24], [25]. Christ et al. [95] thoroughly review and discuss the merits and limitations of the different methods available to analyze polyP in biological samples. Below we highlight some of the options available to characterize polyP in our samples to improve our understanding of the role polyP plays in cartilage tissue formation.

2.5.2.1 Methods of quantification of polyP concentration

When studying polyP metabolism in cells and tissues, it is essential to characterize its concentration in different biological samples, including cells, tissues and fluids. Due to the low

levels of polyP in mammalian cells and tissues, the methods used to quantify polyP in yeast and bacteria cannot be easily adapted for mammalian systems. Current quantification methods used for mammalian cells and tissues have limitations. ^{31}P NMR is a common strategy that can quantify the amount and chain length of polyP, but has low throughput and the protocol is cumbersome which makes it difficult to analyze samples regularly [96]. An enzymatic approach to quantify polyP involves hydrolyzing polyP with *Saccharomyces cerevisiae* exopolyphosphatase followed by orthophosphate quantification, or converting polyP to ATP with *Escherichia coli* polyphosphate kinase and quantifying ATP levels with a luciferase assay. These enzymatic methods were used in the early determination of polyP in mammalian cells and tissues and are highly sensitive, but the enzymes are not yet commercially available [25]. 4',6-diamidino-2-phenylindole (DAPI) has also been used as a fluorometric method for polyP quantification in neurons [97]. DAPI is a commonly used fluorescent probe for DNA that forms a blue complex with an emission peak of 456 nm. The polyP-DAPI complex causes a shift in the emission spectra and fluoresces yellow at a wavelength maxima of 526 nm. This approach requires a high purity of polyP since other biomolecules including nucleotides, RNA, inositol phosphates, and lipids can interfere with the polyP-DAPI fluorescence and lead to misinterpretations [95].

Prior to quantification, several methods require polyP to be extracted from mammalian cells and tissues which can be challenging due to its structural similarity to nucleic acids, vulnerability to enzymatic digestion and hydrolysis (particularly in acidic conditions). Kumble and Kornberg [25] used a phenol/chloroform extraction method followed by nuclease digestion to isolate polyP from rodent tissues. Phenol/chloroform extraction is commonly used for DNA purification since it separates nucleic acids from lipids and proteins. An alternative extraction method involves the binding of polyP to silica spin columns, a method that is also adapted from

techniques available to extract nucleic acids. Recently, a new protocol using silica spin columns for polyP isolation was developed by the Kandel laboratory. This method was designed to extract low levels of polyP from 3D mammalian tissues with minimal loss through the column and subsequently quantified by fluorometry [96]. The tissue samples used in this protocol are similar to those constructed in our system and was therefore the method of choice for quantifying polyP for this project.

2.5.2.2 Methods for the localization of polyP

Imaging can provide information on the localization of polyP within tissue and cell samples without prior extraction methods, as well as qualitative information on polyP content for the comparison of samples with markedly different contents. DAPI is a commonly used fluorophore for imaging polyP, but as mentioned earlier, other biomolecules can interfere with the polyP-DAPI fluorescence signal. JC-D7 and JC-D8 have been identified as novel fluorescent probes that bind specifically to polyP. The JC-D7/D8 probes demonstrate selectivity for polyP and are not sensitive to other biological phosphates, particularly RNA [98]. The dyes are suitable for detecting the localization of polyP and can estimate the levels of endogenous polyP in living cells, however, they are limited to detecting polyP with chain lengths greater than 15 phosphate subunits [98]. They also have been used in a limited number of studies as of yet.

2.5.2.3 Methods for the evaluation of polyP chain length

The chain length of polyP is another parameter that has been investigated to characterize endogenous polyP, albeit less frequently than other parameters. The chain length of polyP can range from tens to several hundred orthophosphate subunits whereby the function of polyP depends on the specific chain length of the polymer [82]. As mentioned above, ^{31}P NMR can be used to provide an estimate of the average chain length of polyP in a sample, but does not provide

insight on chain length distribution. Gel electrophoresis is a method used to determine the average polyP chain length and the chain length distribution in a sample. The gel must be stained with either Toluidene Blue or DAPI for analysis, neither of which stain short-chain polyP and consequently results in a higher average chain length than representative of the sample [95]. Although polyP size ladders are not yet commercially available, DNA size ladders can alternatively be used to estimate the polyP chain lengths [99].

MATERIALS AND METHODS

3.1 Tissue Culture

Cartilage tissue was aseptically excised from the metacarpal-phalangeal joint of cows purchased from a local abattoir (Tom Henderson Meats & Abattoir) within 24 hours of death. The tissue was cultured for two days in Dulbecco's modified Eagle medium (DMEM; 4.5 g/L glucose) supplemented with 1% antibiotic-antimycotic to ensure the absence of microorganism contamination post-dissection. The cartilage tissue was enzymatically digested with 0.2% pronase for 2 hours, then digested with 0.1% collagenase for 48 hours to release chondrocytes. The cells were then seeded on collagen type II coated cell culture membrane inserts at a density of 1×10^6 cells per membrane (12 mm diameter) in Ham's F12 supplemented with 5% fetal bovine serum (FBS) and 1% antibiotic-antimycotic. On day 5 after seeding, the constructs were transferred to DMEM supplemented with 10% FBS, 1% antibiotic-antimycotic, and 100 µg/mL ascorbic acid. DMEM media with glucose concentrations of 1 g/L or 4.5 g/L were used and are referred to as low glucose (LG) and high glucose (HG), respectively. Glucose concentrations of 1 g/L is representative of the approximate physiological levels in synovial fluid, whereas glucose concentrations of 4.5 g/L are supraphysiological and are levels typically used for *in vitro* cultures with high cell density. The volume of media used was either 2 mL or 11 mL, referred to as low volume (LV) and high volume (HV), respectively. Overall, four separate media conditions were tested in the scope of this project: LG-LV, LG-HV, HG-LV, and HG-HV. Select LG-HV cultures were incubated with and without pyruvate and glutamine to test the effects of other nutrients in the media in a preliminary study aimed at informing the next steps of the study. Medium was changed every 2-3 days throughout the culture period.

3.2 Water Content of Cartilage Constructs

Cartilage tissues grown *in vitro* were harvested after different incubation times, washed twice in PBS, and removed from membrane inserts. Tissues were weighed using an electrical balance (AB204-S/FACT; Mettler Toledo) to determine the wet weight, then lyophilized (FreeZone Plus 6; Labconco) overnight and weighed again to determine the dry weight. Water content was calculated as a percentage of wet weight based on the difference between the wet and dry weights.

3.3 Biochemical Composition of Cartilage Constructs

3.3.1 Papain Digests

Tissue samples were digested with papain (40 µg/mL) in a digestion buffer containing 5 mM cysteine HCl and 5 mM EDTA at pH 6.2 for 48 hours at 65°C. Papain digests were kept frozen at -20°C until further analysis.

3.3.2 DNA Content

DNA content of the papain digests was measured using Quant-IT dye binding assay according to instructions from the manufacturer. Fluorometry was carried out with a Synergy H1 plate reader (Biotek) at excitation and emission wavelengths of 480 and 520 nm, respectively. A standard curve was generated using lambda DNA and used to calculate the amount of DNA in the samples.

3.3.3 Sulfated GAG Content

Sulfated GAG content of the papain digests was measured using a dimethylmethylene blue (DMMB) binding assay [100]. Briefly, 10 uL papain digest aliquots were mixed with 200 uL DMMB solution (1.6 mg/mL DMMB in ethanol, 40 mM glycine, 40 mM NaCl, pH 1.25) and quantified spectrophotometrically at 525 nm using a Synergy H1 plate reader. A standard curve

was generated using chondroitin sulfate and used to calculate the amount of sulfated GAG in the sample. Sulfated GAG content was normalized per construct and to DNA content and expressed as µg/construct and µg/µg DNA, respectively.

3.3.4 Collagen Content

The collagen content of papain digests was measured by quantifying the hydroxyproline content [101] which accounts for approximately 10% of the total collagen mass [102]. Papain digest aliquots were subject to acid hydrolysis in 6N HCl at 110°C for 18 hours. The hydroxylates were neutralized in equal volumes of 5.7N NaOH and free hydroxyproline was oxidized with 0.05N Chloramine T, followed by 3.15N perchloric acid, and addition of Ehrlich's reagent. The colour change in the solution was quantified spectrophotometrically at 560 nm with a Synergy H1 plate reader. A standard curve was generated using L-hydroxyproline and used to calculate the amount of collagen in the sample. Collagen content was normalized per construct and to DNA content expressed as µg/construct and µg/µg DNA, respectively.

3.3.5 Advanced Glycation End Products (AGE) Content

AGE content of the papain digests was quantified fluorometrically at excitation and emission wavelengths of 360 and 440 nm, respectively, to estimate the number of crosslinks in the tissue [103]. A quinine standard curve (0-1.4 µg/mL) was generated to calculate the amount of AGE's in the sample. The results are normalized to collagen content and expressed as ng of quinine/mg collagen.

3.4 Histology

Histological evaluation was performed by the Louise Pelletier histology core facility. Samples were fixed in 10% formalin for 72 hours then placed in 70% ethanol. Tissues were embedded in

paraffin and sectioned to 4 µm thickness. Histological sections were dewaxed in xylene, rehydrated sequentially by replacing xylene by ethanol and ethanol by diH_2O and stained with Alcian blue to detect proteoglycans and Picosirius red to detect collagens. The tissues were visualized by an Axio Scan.Z1 microscope using a Plan-Apochromat 20X objective and a brightfield channel.

3.5 Height Measurements and Mechanical Properties of Cartilage Constructs

The height of the tissues was measured using a Mach 1 mechanical tester (Biomomentum). The height was zeroed at the surface of the sample holder. Tissues were removed from the insert and oriented perpendicular to the indentation axis on the sample holder. The height was determined when the indenter contacted the surface of the tissue at a force of 0.001 N.

Mechanical properties were measured by performing indentation tests to determine the stiffness of the tissue. After determining the height of the tissue, samples were submerged in media. Starting at the surface of the tissue, a 1 mm diameter spherical indenter was pressed into the sample at 0.05 mm/s up to 10% strain using a 0.25 N load cell and recorded at a frequency of 2.5 kHz. The resulting displacement and load were recorded by the Mach 1 mechanical tester (Biomomentum) and analyzed based on Hayes' model that is applicable for an elastic layer placed on a flat rigid surface assuming limited sliding at the interface and considers the spherical geometry of the indenter [104]. The Young's modulus was computed based on the calculated stress-strain curve generated from the force-displacement data.

3.6 Determination of Metabolites in Cartilage Constructs and Culture Media

3.6.1 Glucose Content in Media

Media samples were collected at various time points during tissue culture and frozen at -20°C until quantified. Glucose content was quantified based on the spectrophotometric hexokinase (HK) assay [105]. Briefly, 20 µL of media samples were mixed with 100 µL HK assay reagent (Tris $MgCl_2$ pH 7.5, HK, glucose-6-phosphate dehydrogenase, NAD, and ATP). The plate was incubated at room temperature for 15 minutes and the absorbance at 340 nm was measured using a Synergy H1 plate reader. A standard curve was generated with DMEM (0-0.5 g/L) and used to calculate the concentration of glucose in the samples. The glucose consumption rate over the first 24 hours after a media change was calculated by normalizing glucose consumed over time by the DNA content and expressed as mg/hr/µg DNA.

3.6.2 Lactate Content in Media

Lactate content was measured from media samples collected on day 7 6 hours and 48 hours after a media change. Media samples were filtered using Amicon Ultra-2 Centrifugal Filter Units (Millipore) to remove serum with potential endogenous enzyme activity. Lactate was measured using a colorimetric Lactate Assay Kit (Sigma) based on the oxidation of lactate catalyzed by lactate dehydrogenase, where NADH reduces MTT according to manufacturer instructions. Briefly, 20 µL of media samples was mixed with 80 µL of reaction mix and the absorbance at 565 nm was measured using a Synergy H1 plate reader. The absorbance was read immediately after addition of the reaction mix and again after a 20 minute incubation at room temperature. A standard curve of L-Lactate (0-1 mM) was prepared in culture medium without serum and the difference in absorbance readings was used to calculate the concentration of lactate in the media samples. The lactate concentration in the well was expressed as mM and the lactate released from the tissues

was expressed as mmol/well. Lactate content was also analyzed as a ratio of glucose consumed expressed as mmol lactate/mmol glucose.

3.6.3 ATP Content in Cartilage Constructs

ATP content was measured according to modifications on a previously published protocol [106]. Briefly, cartilage constructs were washed twice in PBS, harvested, weighed, and immediately placed in 0.5 mL 1% phosphatase inhibitor cocktail in diH2O (P5726; Sigma-Aldrich) to prevent ATP digestion. Samples were placed in a boiling water bath for 10 minutes to extract ATP. The extract was centrifuged at 12 000 g for 5 minutes and the supernatant was collected. ATP content of the supernatant was quantified using the Sigma FLAA ATP Bioluminescent assay kit according to manufacturer instructions. Briefly, 100 µL of the supernatant was mixed with 100 µL of assay mix containing luciferase, luciferin, $MgSO_4$, DTT, EDTA, BSA, and tricine buffer salts. The light produced was measured immediately using a Synergy H1 plate reader and is proportional to the ATP content. A standard curve ($8x10^{-8}$-$8x10^{-5}$ mol/L) was generated to calculate the amount of ATP in the samples and expressed as nmol ATP/mg wet weight.

3.6.4 PolyP Content in Cartilage Constructs and Media

PolyP quantification was performed with modifications to the method developed by the group of Dr. Rita Kandel [96]. Briefly, cartilage constructs and media samples were digested with proteinase K (1 mg/mL) in a buffer containing 10 mM EDTA and 10 mM Tris pH 8 for 2 hours at 56°C to release polyP from the tissue. The tissue digest was loaded on a silica spin column (Qiagen) to isolate polyP. The eluent was treated with 10 U DNase I (Millipore Sigma) and 2.5 U RNase A (Millipore Sigma) to eliminate nucleic acids that can cause extraneous fluorescence signals. PolyP was quantified fluorometrically with 50 µg/mL DAPI (Sigma Aldrich) in diH_2O at excitation and emission wavelengths of 415 and 558 nm, respectively. A standard curve of polyP-

45 (1-60 µM) was generated to determine polyP levels in the samples. Our results were at odds with those reported by Lee et al. [96] and the method was evaluated substantially (see Appendix I).

Localization of polyP in cartilage constructs was visualized using histological sections as described above. After dewaxing and rehydration, the tissues were stained with DAPI (5 µg/mL in diH_2O) for 5 minutes. When bound to polyP, the emission peak of DAPI shifts from 456 to 526 nm. The fluorescence was visualized by a Zeiss epifluorescence microscope using a 49 DAPI filter set (Zeiss) to image DNA and a 70 HE Alexa Fluor 430 filter set (Zeiss) to image polyP. Selected tissues were digested with 15 U of alkaline phosphatase (ALP) (Millipore Sigma) in a buffer containing 6 mM Tris/HCl, 6 mM $MgCl_2$, and 0.12 mM ZnCl, pH 9, for 1 hour to digest polyP. Images were analyzed with FIJI by selecting the tissue in the image and measuring the area, integrated density and mean gray value of the tissue. The total corrected tissue fluorescence (TCTF) = integrated density – (area of selected tissue x mean fluorescence of background reading) was calculated to determine the fluorescence intensity of the tissue [107].

3.6.4 Exopolyphosphatase Activity

Cartilage constructs were harvested and washed twice in PBS. Proteins were extracted from the tissues and assessed for exopolyphosphatase activity based on a previously published protocol [90]. The tissues underwent three freeze-thaw cycles in a homogenization buffer containing 50 mM Tris-HCl (pH 7.5), 10 mM $MgCl_2$, 0.5 mM EDTA, 150 mM NaCl, and 0.2% vol/vol TritonX-100. After the third thaw, tissues were mechanically homogenized. The solutions were centrifuged at 14 000 g for 15 mins and the protein content of the supernatant was determined using a Pierce BCA protein assay (Thermo Fisher Scientific). For each sample, a reaction mixture was prepared containing 25 µg of protein and 0.4 µmol sodium phosphate glass (polyP) for a final volume of

200 µL. To account for phosphate content of protein extracts and hydrolysis of sodium phosphate glass, reactions mixtures of only protein from each sample or only polyP were also prepared in the same buffer for a final volume of 200 µL. The reaction mixtures were incubated at 37°C for 24 hours. The phosphate produced by enzymes with exopolyphosphatase activity during the incubation period was quantified spectrophotometrically. Phosphate content was measured by reacting samples with a 1:6 solution of 10% ascorbic acid and 0.42% ammonium molybdate in 1N H_2SO_4 for 1 hour at 37°C. The acidic solution of ammonium molybdate reacts with phosphate to produce phosphomolybdic acid. The acid is reduced in the presence of ascorbic acid and a resulting blue colour is quantified spectrophotometrically at 620 nm with a Synergy H1 plate reader. A standard curve was generated with sodium phosphate dibasic (0-0.5 mM) in the homogenization buffer with triton-X and bovine serum albumin at protein levels equivalent to those of the diluted samples. Exopolyphosphatase activity was analyzed by subtracting the Pi content of polyP only samples and protein only samples from samples with polyP and protein. The activity was normalized to the amount of protein in the reaction and expressed as mM/24hours/mg.

3.7 Formation of 3D Printed Moulds and Polydimethylsiloxane Inserts

Inserts of various shapes and sizes were designed using Fusion 360 software and printed from Phrozen sonic 8K stereolithography 3D printer with Aqua Gray 8K resin. The 3D printed moulds were washed twice in isopropanol, the first wash in an ultrasonic and the second wash in a stirring wash bath, and then UV cured for 1 hour.

Polydimethylsiloxane (PDMS) was prepared using the Sylgard^{TM} 184 Silicone Elastomer Kit by mixing the monomer with curing agent in a 1:10 w/w ratio and degassed in a vacuum for 30 minutes. PDMS was cast onto 3D printed moulds and cured at 90°C for 15 minutes. The PDMS inserts were demoulded from the 3D prints and processed for biofunctionalization.

Surface modification of the PDMS inserts was conducted with oxygen plasma treatment for 30 seconds at 50%, 7 sccm to improve surface wettability. PDMS inserts were coated with 0.01% polydopamine w/v in 10 mM Tris-HCl (pH 8.5) for 1 hour. The inserts were subsequently coated with collagen type II and UV sterilized for 30 minutes.

3.8 Statistical Analysis

All experiments were repeated three times using cells isolated from different animals unless specified otherwise. One-way analysis of variance (ANOVA) with Tukey's *Post hoc* test was used for experiments conducted with more than 2 conditions to determine significance ($p \leqslant 0.05$). When the Levene's test was significant, the Games-Howell *Post hoc* test was used. Student's t-test was used for experiments conducted with 2 conditions to determine significance ($p \leqslant 0.05$). Each test was performed with technical triplicates. Data are expressed as mean ± standard deviation (SD).

RESULTS AND DISCUSSION: PART 1

4.1 Stability of nutrient environment over time

One of the underlying objectives of this project was to determine whether an adjustment in the glucose concentration in the media can be maintained by increasing the volume. To investigate this question, it was necessary to make adjustments to the culture system that would result in more uniform culture conditions over time. In this study, this was approached by increasing the culture media volume used for cultures, without changing the hydrostatic pressure in the system. To test the effect of increased media volume on the stability of the nutrient environment in the cultures, we quantified the levels of glucose in the media over time between two media changes at different time points over the course of a 4 week culture period for cultures under the 4 conditions detailed in the methods, namely LG-LV, LG-HV, HG-LV, and HG-HV (LG = 1.0 g/L glucose or low concentration; HG = 4.5 g/L glucose or high concentration; LV = 2 mL of medium or low volume; HV = 11 mL of medium or high volume). Glucose content in the culture media was measured 0 hours, 6 hours, 24 hours, and 48 hours after the media changes carried out at days 0, 7, 14, and 21 during the culture period. On day 0, no significant difference in glucose content in the media was observed for all conditions between 0 and 48 hours after media change (Figure 4A). At this time in culture, the chondrocytes are adjusting to the new medium and nutrient environment and are in the initial stages of processes that involve proliferation and ECM deposition. On day 7, glucose content in the LG-LV media decreased by 92.7±0.8% at 48 hours after the media change, whereas the LG-HV media lost 45.2±10.2% of the glucose content (Figure 4B). These results indicate that increasing the volume of low glucose-containing media offers an improvement in nutrient stability but is not completely stable over 48 hours representing the typical period between two media changes. In comparison, glucose content decreased by 42.1±8.8% in HG-LV and 6.6±7.6% in HG-

HV between 0 and 48 hours after media change on day 7. Of note, the decrease in glucose concentration over 48 hours observed at days 14 and 21 was comparable to that measured at day 7 (Figure 4C-4D). This result suggests that either cell proliferation stops after 7 days or that average glucose uptake per cell decreases after that time point.

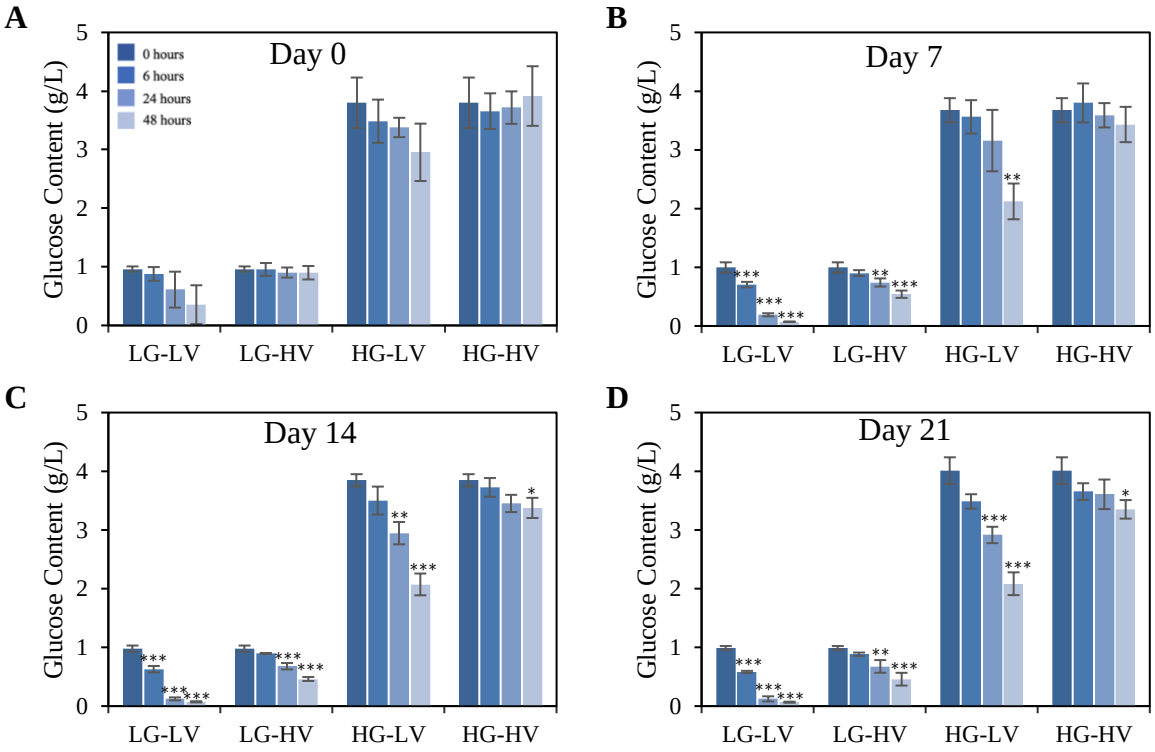

Figure 4. Glucose content in media incubated with high density chondrocyte cultures 0, 6, 24, and 48 hours after media change on **(A)** day 0, **(B)** day 7, **(C)** day 14, and **(D)** day 21 of the culture period. LG = low glucose; HG = high glucose; LV = low volume; HV = high volume. Experiments were repeated 3 times with cells isolated from different animals. Data are represented as mean ± SD. Statistically significant decrease in glucose concentration compared to 0 hours is denoted by *($p<0.05$), **($p<0.01$), ***($p<0.001$).

Overall, the use of higher media volume provides an improvement in maintaining a less variable nutrient environment for tissue cultures; however, the conditions investigated do not prevent fluctuations in glucose concentration completely, particularly when using a physiological

initial concentration of glucose. Increasing media volumes further is possible but would be prohibitive from a cost perspective and associated with technical challenges in the selection of adequate plasticware for the cultures. Subsequent results should be interpreted in the context of these observations.

4.2 Biochemical composition of cartilage constructs

The biochemical composition of the cartilage constructs was characterized by quantifying levels of DNA, sGAG, collagen, and water content on days 7, 14, and 28 of culture under the four specific conditions. The DNA content of tissues is representative of the number of chondrocytes in the construct and will provide an indication of how culture conditions affect the number of cells in culture which is impacted by proliferation and cell death. As can be seen in Figure 5, constructs cultured in low volumes of media (LV) exhibit statistically significant increases in DNA content in both glucose concentrations (LG and HG) compared to the content at day 0, but the DNA content plateaus at 14 days. Conversely, in the two HV conditions, the DNA content continues to increase throughout the culture period with a significant increase observed at 28 days compared to days 0 and 7.

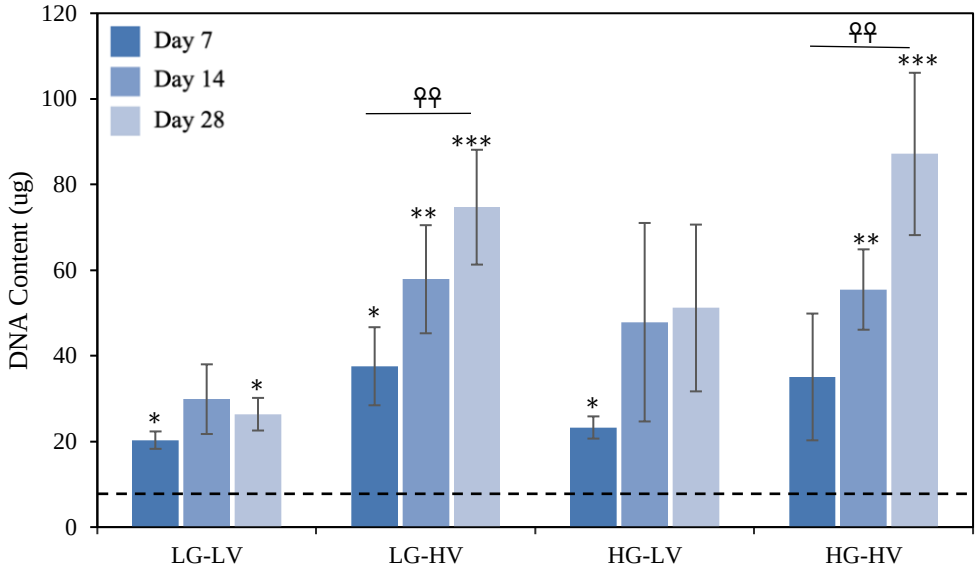

Figure 5. DNA content of cartilage constructs at day 7, 14, and 28 in culture. LG = low glucose; HG = high glucose; LV = low volume; HV = high volume. The dotted line represents average DNA content of cartilage constructs at day 0. Experiments were repeated 3 times with cells isolated from different animals. Data are represented as mean ± SD. Statistically significant increase in DNA content compared to day 0 is denoted by *($p<0.05$), **($p<0.01$), ***($p<0.001$). Statistically significant increase in DNA content compared to day 7 of the same condition is denoted by ♀♀($p<0.01$).

ECM accumulation in the *in vitro*-formed tissues can be evaluated by measuring the levels of sGAG and collagen in the constructs and can provide an indirect estimate of the tissue functionality, which is to say its ability to withstand the complex loads of the joint. Figure 6A illustrates that increasing the media volume significantly increases the total amount of sGAG content in the constructs. At low volumes, the HG construct contained significantly higher levels of sGAG than the LG construct, however, no difference in sGAG levels was measured between the different glucose concentrations reported for HV. These results are supported by a previous study that investigated glucose supplementation as an alternative to high media volumes [71].

When normalized to DNA content, the LG-HV condition remains significantly greater than the LG-LV, however, the HG condition is not significantly impacted by an increase in volume (Figure 6B). It has been reported that proteoglycan accumulation is favored in high volumes of low glucose containing media, yet the underlying mechanisms remain unclear [108]. sGAG content of articular cartilage is reported to comprise ~2.5-10% of the tissue wet weight [109], [110], meanwhile our engineered constructs ranges from 0.4-1.5% wet weight with the highest values reported for the LG-HV construct at day 28. Our results indicate that HV is preferred for proteoglycan accumulation; however, we did not see a notable effect from the low (i.e. physiological) glucose concentration condition compared to the high (i.e. supraphysiological) glucose concentration condition.

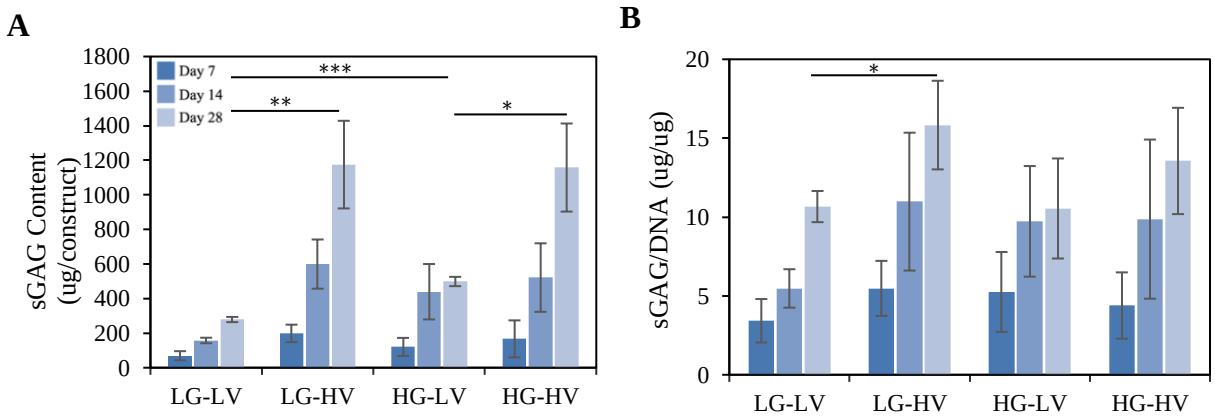

Figure 6. (A) Total sGAG content of cartilage constructs and **(B)** sGAG normalized to DNA content at day 7, 14, and 28. LG = low glucose; HG = high glucose; LV = low volume; HV = high volume. Experiments were repeated 3 times with cells isolated from different animals. Data are represented as mean ± SD. Statistically significant increase in sGAG content compared to LV is denoted by *($p<0.05$), **($p<0.01$), ***($p<0.001$).

Similar trends were observed for collagen content as in sGAG content. Figure 7A illustrates that total collagen levels in the construct were significantly greater in the HV constructs; however, no significant changes were observed when normalized to DNA. Interestingly, when normalized

to DNA, the HG-LV condition had significantly more collagen than the LG-LV condition (Figure 7B). Previous studies have reported that collagen accumulation is favoured in high glucose-containing media [108]. In articular cartilage, collagen comprises up to 30% tissue wet weight [109], [110] compared to 0.3-1.2% synthesized in our cartilage constructs. The types of collagen expressed in the constructs was not investigated for this project and would be of interest to develop a deeper understanding of the composition of the tissue. Indeed, more collagen content does not necessarily signify that the right type of collagen is being produced.

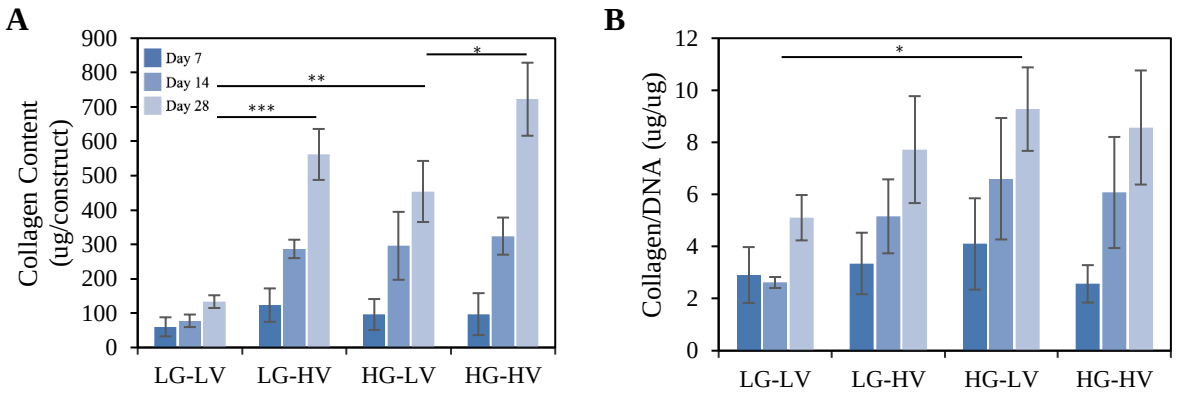

Figure 7. (A) Total collagen content in cartilage constructs and **(B)** collagen normalized to DNA content for days 7, 14, and 28. LG = low glucose; HG = high glucose; LV = low volume; HV = high volume. Experiments were repeated 3 times with cells isolated from different animals. Data are represented as mean ± SD. Statistically significant increase in collagen content compared to LV is denoted by *($p<0.05$), **($p<0.01$), ***($p<0.001$).

The collagen-to-sGAG ratio often dictates the tissue stiffness [111] and was calculated in our cartilage constructs as illustrated in Figure 8. A higher ratio may be indicative of stiffer tissue, whereas a lower ratio may be indicative of softer tissue. Interestingly, the collagen-to-sGAG ratio in HG-LV was significantly greater than the three other conditions. The collagen-to-sGAG ratio in native tissue is often greater than 3-to-1 [112], yet the ratio in our constructs were all below 1-to-1. The collagen-to-sGAG ratio in tissue engineered constructs is often lower than native

cartilage. This discrepancy can be explained by the lower collagen content in the engineered constructs compared to native tissue. Studies have investigated different strategies to selectively increase collagen content more than sGAG content to achieve ECM ratios that are comparable to native cartilage [112].

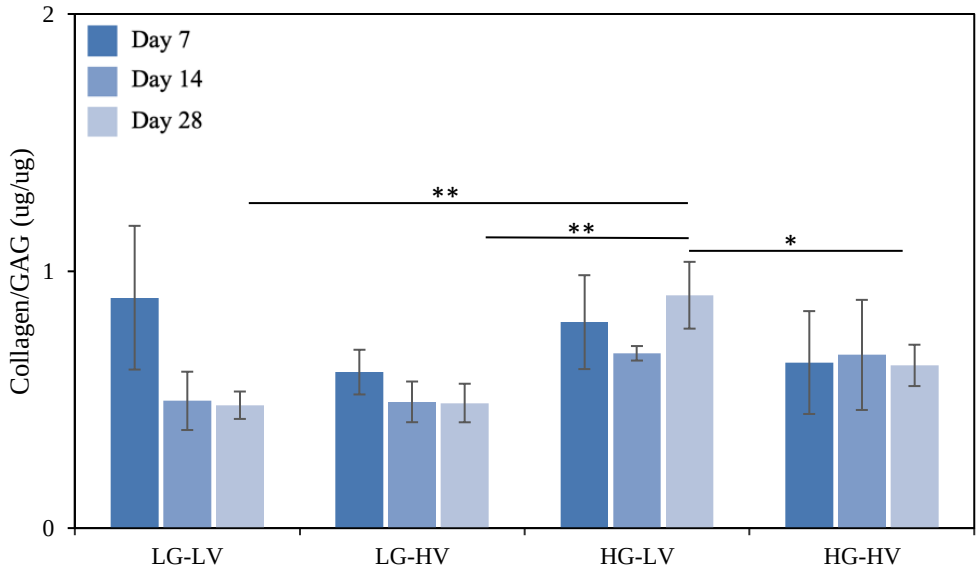

Figure 8. Collagen-to-sGAG ratio of cartilage constructs at day 7, 14, and 28. LG = low glucose; HG = high glucose; LV = low volume; HV = high volume. Experiments were repeated 3 times with cells isolated from different animals. Data are represented as mean ± SD. Statistically significant increase in collagen-to-sGAG ratio is denoted by *($p<0.05$), **($p<0.01$).

Another component that was quantified in the cartilage constructs was the presence of advanced glycation end products (AGEs). AGEs are modifications of lipids or proteins that become glycated and are prone to develop and accumulate in hyperglycemic conditions. AGEs can accumulate in all tissues of the body and form cross-links between ECM proteins, which can alter the mechanical properties of the tissue. In cartilage tissue, increased levels of AGE cross-links can cause stiffening of the collagen network, decreased proteoglycan synthesis, and degradation of the ECM [113], [114]. These AGE-induced negative effects on cartilage can render

the tissue susceptible to mechanical failure and contribute to the development of OA. In our system, no major differences in AGE levels were reported between the tissues cultured under the four different media conditions (Figure 9).

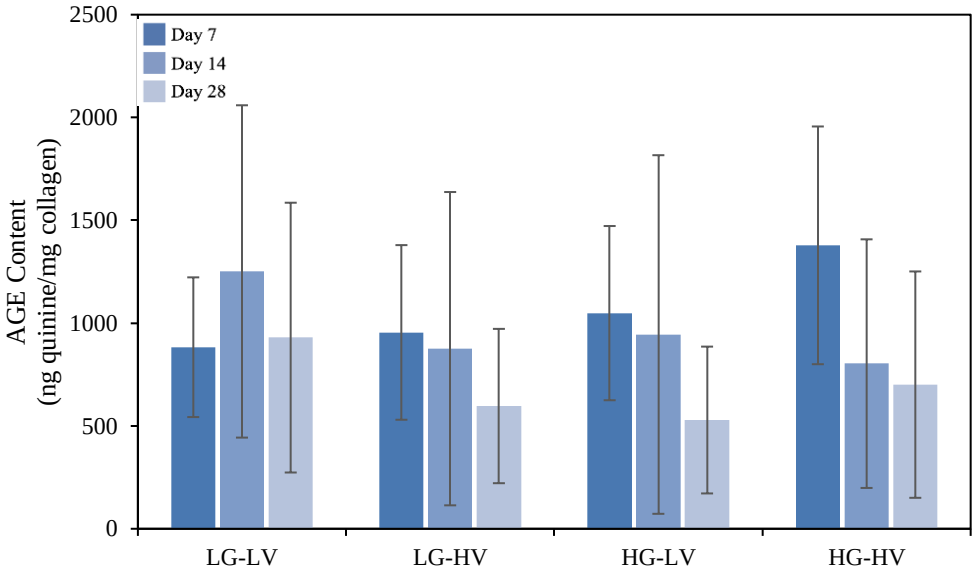

Figure 9. AGE content of cartilage constructs at day 7, 14, and 28. LG = low glucose; HG = high glucose; LV = low volume; HV = high volume. Experiments were repeated 3 times with cells isolated from different animals. Data are represented as mean ± SD.

The fluid phase is the primary component of cartilage and is reported to make up 80% of the tissue wet weight [27]. The water content of the constructs ranged between 87-93% and no differences were observed between the culture conditions (Figure 10). The higher water content in our engineered constructs compared to native cartilage suggests that the matrix of the engineered constructs suggests substantial compositional and structural differences compared to native matrix and might be a result of the relatively low collagen-to-sGAG ratio observed within *in vitro*-formed tissues compared to native cartilage. The differences in matrix composition will also impact the mechanical properties. The lack of differences in water content between the different conditions

may be due to a lack of differences in the number of crosslinks in the tissue that was determined based on the AGE content reported above.

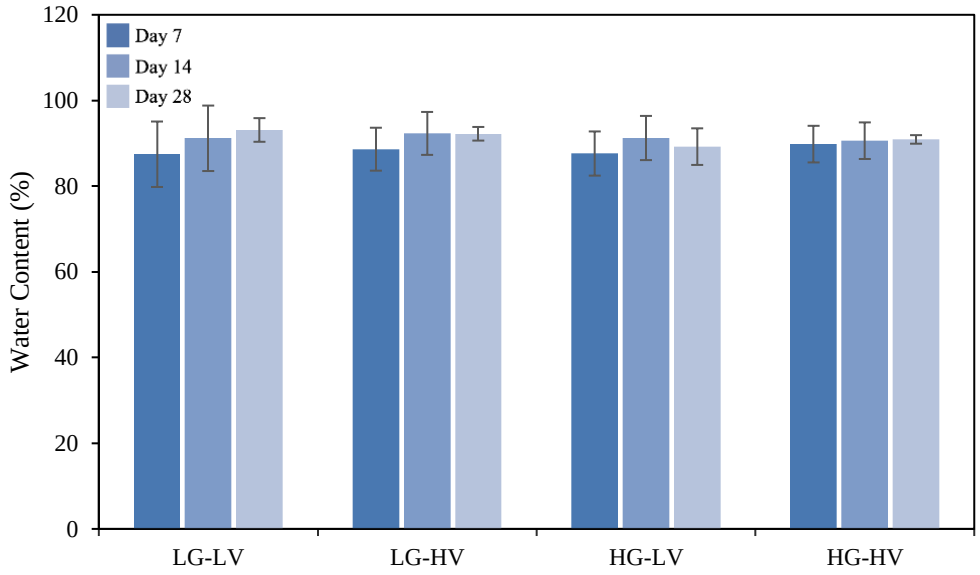

Figure 10. Water content of cartilage constructs at day 7, 14, and 28. LG = low glucose; HG = high glucose; LV = low volume; HV = high volume. Experiments were repeated 3 times with cells isolated from different animals. Data are represented as mean ± SD.

The results presented thus far indicate that increasing the media volume has a greater impact on matrix accumulation for LG conditions than HG. We speculate that the initial HG concentrations can supplement for the lower volume condition and maintain a stable glucose environment for a longer time period. Overall, the accumulation of ECM components is favoured in high media volumes, but physiological glucose concentrations did not provide additional benefits for the metrics evaluated.

Histological evaluation of the constructs was conducted in order to visualize the morphology of the tissue. Tissues harvested at day 28 were dyed with Alcian blue that stains sulfated GAGs and glycoproteins, and Sirius red that stains collagens (Figure 11). The matrix staining intensity and apparent thickness of the tissues illustrate similar trends in sGAG and

collagen content of the different media conditions as those reported from the quantification methods of ECM components. To note, the LG-HV construct illustrates a homogenous cellular profile, whereas the other constructs have a higher cell density at the bottom of the construct in proximity to the membrane. In our study, the LG-HV media may provide a suitable environment for constructs to generate these uniformities by means that remain unclear. While the LG-HV tissue appears homogenous, the surface of the tissue is uneven compared to other conditions. The chondrocytes of the LG-HV construct also appear more spherical compared to other constructs; however, this should be confirmed with quantitative analysis. Nevertheless, these observations could be an indication of the benefits of providing more physiological culture conditions (e.g. glucose levels) at the cellular level. As well, at day 28, the differences in tissue thickness are evident between the LV and HV conditions. To confirm this observation, quantitative evaluation of tissue thicknesses was obtained using a Mach 1 mechanical tester. In LG media, the height of the HV construct was significantly greater than the LV construct, whereas in HG media, increasing the media volume did not significantly impact the height of the tissue (Figure 12). No significant differences in height were observed between the LG and HG conditions in HV medium.

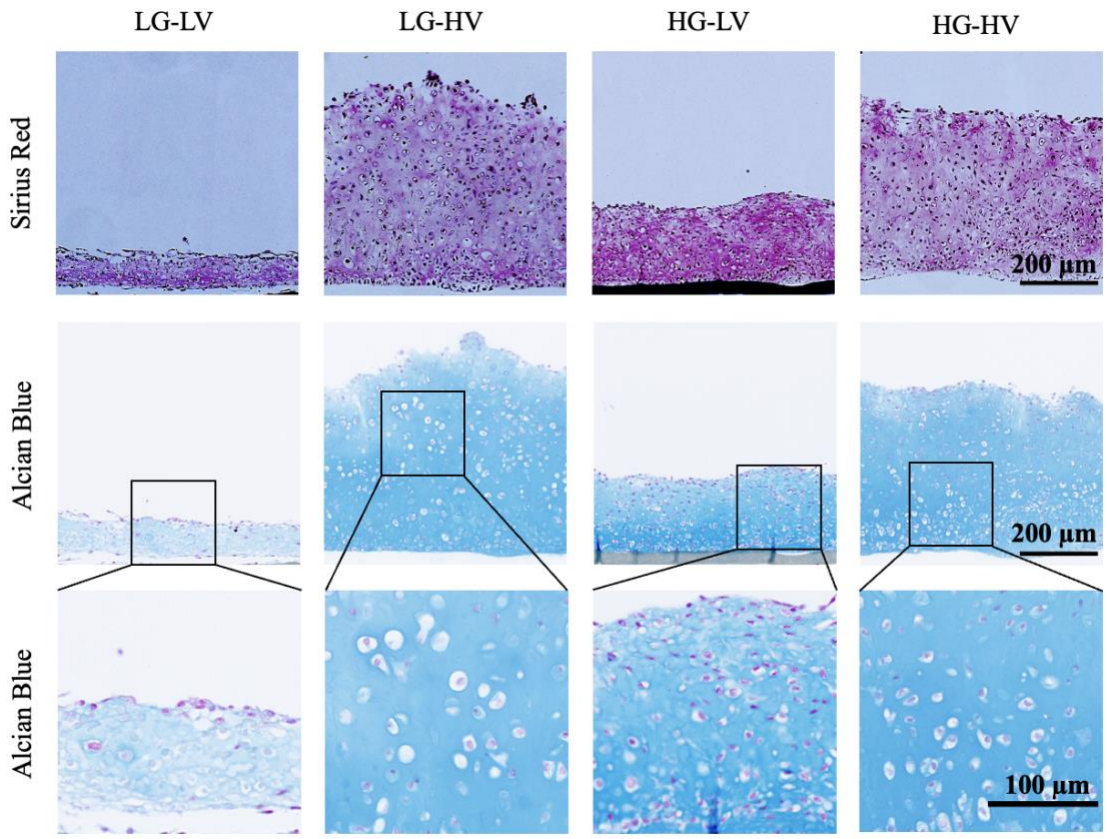

Figure 11. Histological sections of cartilage constructs stained with Alcian Blue and Sirius Red on day 28. LG = low glucose; HG = high glucose; LV = low volume; HV = high volume.

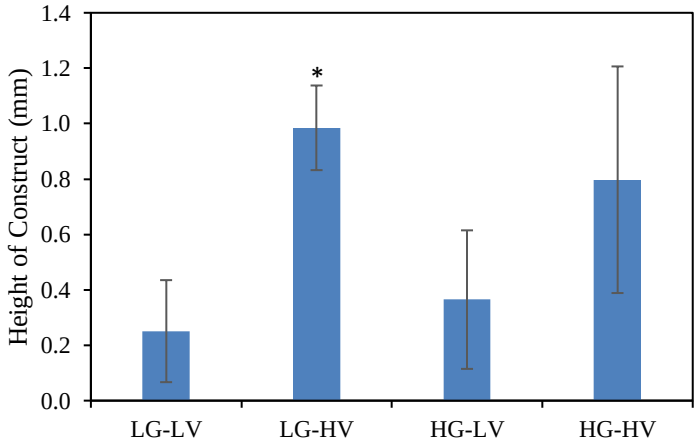

Figure 12. Height of cartilage constructs on day 28. LG = low glucose; HG = high glucose; LV = low volume; HV = high volume. Experiments were repeated 3 times with cells isolated from different animals. Data are represented as mean ± SD. Statistically significant increase in height compared to LG-LV is denoted by *($p<0.05$).

4.3 Mechanical properties

As a load-bearing tissue, it is fundamental that the engineered constructs can withstand regular cycles of load experienced by native cartilage within the joint. To evaluate the mechanical properties of the constructs, indentation tests were conducted to measure the stiffness of the tissue. An indentation test works by displacing a spherical indenter against the tissue perpendicular to the surface and recording the load as a function of displacement. The material stiffness is calculated based on stress-strain curves generated from the force-displacement data. Our results summarized in Figure 13 indicate no significant differences between the constructs with stiffness ranging between 0.084 and 0.221 MPa. The Young's modulus of native cartilage has been reported to range from 0.45-0.80 MPa [28]. The Young's modulus of our engineered constructs is lower than native values which suggests our constructs are softer. This finding is also supported by the lower collagen-to-GAG ratio and higher water content of our constructs compared to native cartilage. As well, the trends in stiffness of the four conditions support the data presented in the collagen-to-GAG ratio where the HG-LV condition had a significantly greater ratio than the other three conditions. This ratio offers an initial indication of the mechanical stiffness of the tissue. However, these interpretations of the data remain provisional because several issues became apparent when conducting the indentation tests that may have impeded the accuracy of our results. For example, the surface of the tissue was uneven, therefore the tip of the indenter may not have been in full contact with the sample. As well, our tests had low signal-to-noise ratios, in part because of the material softness and because of the contact area which could not be addressed because of surface non-uniformities, and issues with the model fit of the data were also observed, which indicates that the calculated Young's modulus may have been extrapolated inaccurately from the model. Future

work is needed to develop a standardized protocol in our lab that will accurately measure the complex mechanical properties of the engineered constructs.

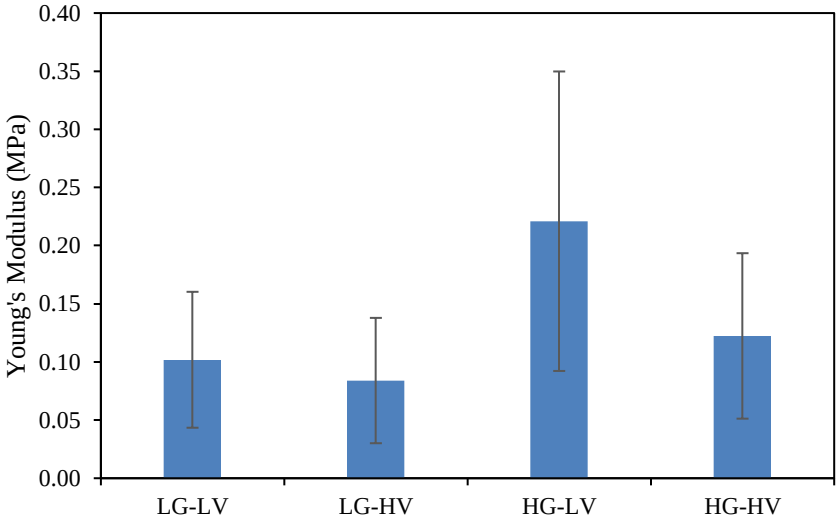

Figure 13. The stiffness of cartilage constructs recorded from indentation tests at 10% strain. LG = low glucose; HG = high glucose; LV = low volume; HV = high volume. Experiments were repeated 3 times with cells isolated from different animals. Data are represented as mean ± SD.

RESULTS AND DISCUSSION: PART 2

5.1 Glucose consumption, lactate release, and ATP production

Next, we were interested in understanding the impact of glucose concentration on the levels of key bioenergetic molecules in chondrocytes. In order to investigate the metabolic pathways conducted in chondrocytes, glucose uptake and metabolites content including lactate and ATP were quantified in the cartilage constructs, as well as their media. First, the rate at which glucose was consumed by a cell over the initial 24 hours after media change in the samples reported in Figure 1 was calculated (Figure 14A). Unexpectedly, these data illustrate that glucose is consumed at comparable rates across all four conditions and all three time points. This suggests that, in our system, glucose concentration does not affect the uptake rate. Also, glucose consumption rate between time points on day 7 reported a significant decrease between 24-48 hours compared to 6-24 hours for the LG-LV condition which suggests an effect of glucose depletion (Figure 14B).

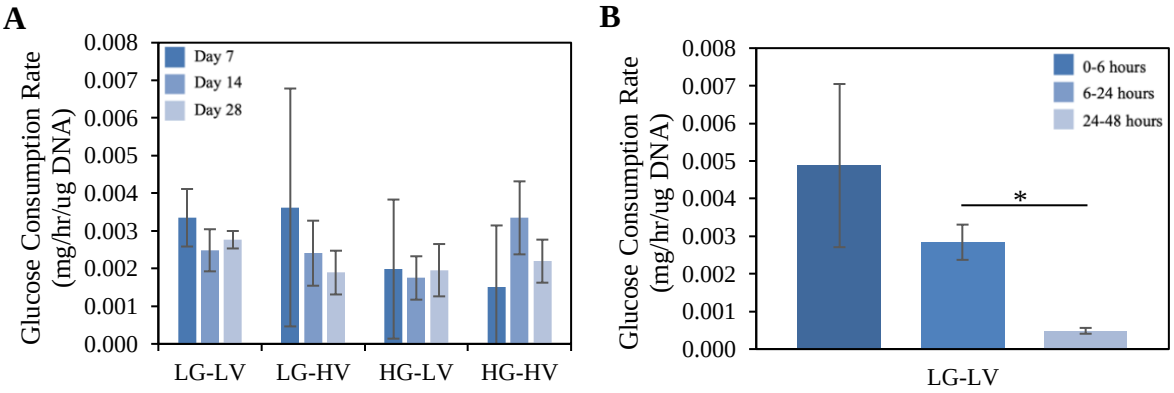

Figure 14. (A) Glucose consumption rate of constructs during the first 24 hours after media change on day 7, 14, and 28. **(B)** Glucose consumption rate of LG-LV constructs on day 7 between 0-6 hours, 6-24 hours, and 24-48 hours. LG = low glucose; HG = high glucose; LV = low volume; HV = high volume. Experiments were repeated 3 times with cells isolated from different animals. Data are represented as mean ± SD. Statistically significant difference in consumption rate is denoted by *($p<0.05$).

Next, new cartilage constructs were cultured for 7 days and harvested either 6 hours or 48 hours after media change. The two time points were chosen to compare the metabolic state when glucose is available in the media at levels near those initially introduced with the media change i.e. after 6 hours, and just before the following media change when substantial depletion has taken place, particularly for the LG-LV condition i.e. after 48 hours. After 48 hours, total glucose uptake of the constructs was comparable for all four media conditions as a result of comparable consumption rates (Figure 15A). Consequently, as mentioned above, the glucose content in LG-LV media likely depletes before the following media change and may explain why the matrix accumulation is significantly lower for this construct than the other three conditions.

Lactate is a metabolic waste product of glycolysis that is released from chondrocytes into the extracellular environment. Lactate production offers an indication that pyruvate did not enter the tricarboxylic acid (TCA) cycle and supports the notion that chondrocytes *in vivo* rely mostly on glycolysis for energy production and not oxidative phosphorylation [73]. Lactate concentrations were significantly higher in LV media compared to HV media in both LG and HG conditions ($p<0.001$) (Figure 15B). At low volumes, the lactate concentration was significantly higher in HG media compared to LG media ($p<0.01$). Greater lactate concentrations in LV conditions may lead to acidic conditions which can be harmful for cell viability [73] and may explain why higher volumes are superior for tissue growth. Although lactate concentration was inversely proportional to media volume, the total lactate content released by chondrocytes was significantly higher with increased media volume (Figure 15C). The greater amount of total lactate content in HV conditions attributes to the fact that there are also more cells in these conditions. Figure 15D illustrates the ratio of lactate released to glucose consumed is greater than 2. The medium used for these experiments was supplemented with pyruvate and glutamine. Pyruvate can be converted to lactate

at a 1:1 ratio and may have contributed to lactate content quantified in the media, potentially influencing the lactate release/glucose uptake ratio. The impact glutamine has on the levels of lactate in the media is unknown at this time. Until we decipher how pyruvate and glutamine influence lactate content in the media, we cannot yet speculate that most of the glucose is being converted to lactate through anaerobic processes [71]. Chondrocytes may also be relying on internal carbon sources, likely glycogen [102], which is then converted to lactate through glycolysis [78].

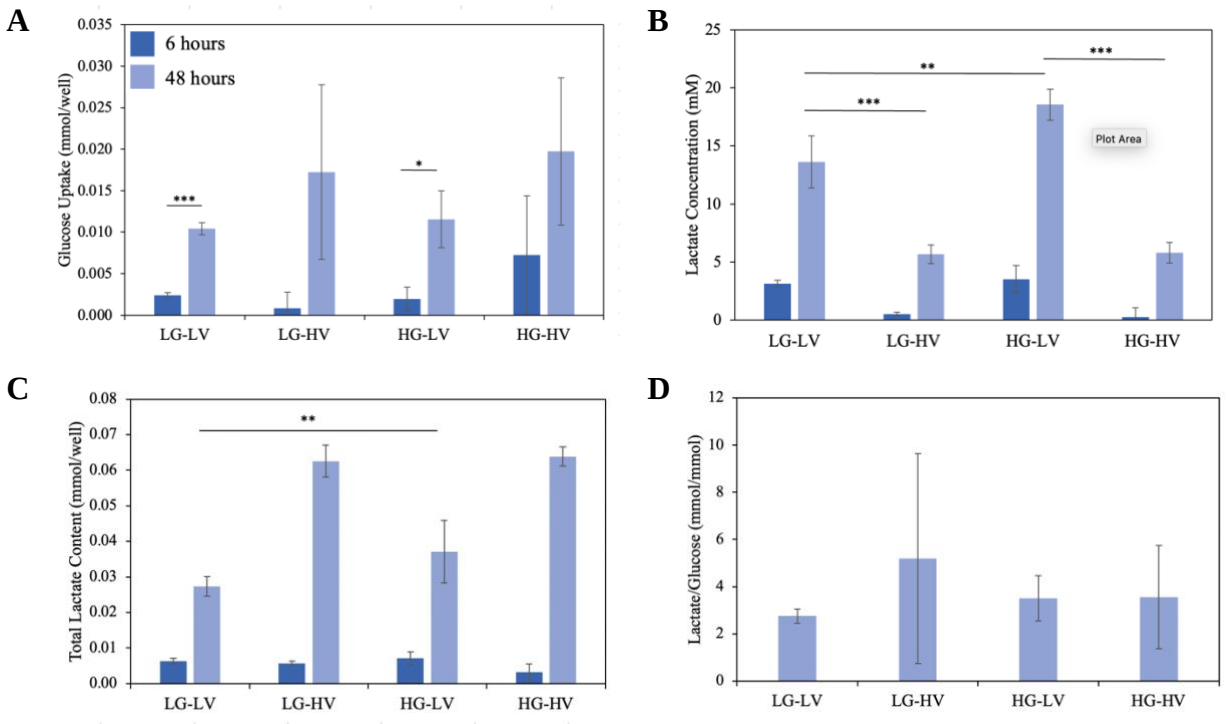

Figure 15. (A) Total glucose uptake, **(B)** lactate concentration, and **(C)** total lactate content of cartilage constructs on day 7 6 hours and 48 hours after media change. **(D)** Total lactate content to glucose uptake ratio of cartilage constructs on day 7 48 hours after media change. The ratio at 6 hours was not reported due to high variance levels at that time point. LG = low glucose; HG = high glucose; LV = low volume; HV = high volume. Experiments were repeated 3 times with cells isolated from different animals. Data are represented as mean ± SD. Statistically significant difference between conditions is denoted by *($p<0.05$), **($p<0.01$), ***($p<0.001$).

Total ATP content in digests from the tissue construct was significantly higher in HV than LV at 6 hours after media change for LG constructs ($p<0.01$) and at 48 hours after media change for HG constructs ($p<0.05$) (Figure 16A). Here we speculate that the difference observed between LG-LV and LG-HV at 6 hours could be due to a higher availability of glucose in HV, but it is unclear why this difference does not exist at 48 hours. LG-LV may be relying on reserves of other bioenergetic molecules for ATP synthesis. As for the HG conditions where an excess of glucose exists in the media, the difference observed at 48 hours may be caused by an accumulation of metabolites that inhibit ATP synthesis in the HG-LV condition. When normalized to wet weight, no significant differences were reported between conditions at either time point (Figure 16B). The constructs from our system generated an average of 0.09±0.03 nmol/mg wet weight compared to previous studies that reported 0.7 nmol/mg wet weight in native bovine cartilage plugs [115]. It is well supported that ECM synthesis rates are closely related to ATP availability [78], [79], [116], therefore, our engineered constructs may have slower biosynthetic activity than native cartilage

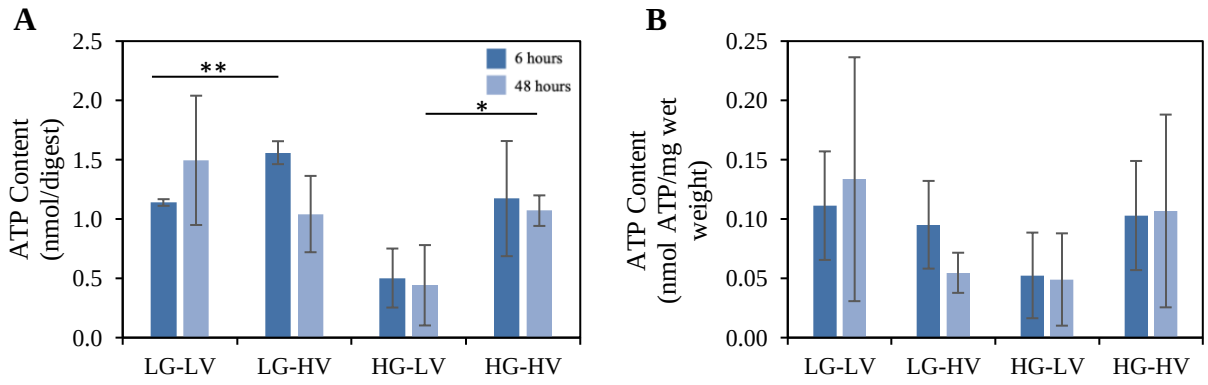

Figure 16. (A) Total ATP content in digest and **(B)** ATP content normalized to wet weight on day 7 6 hours and 48 hours after media change. LG = low glucose; HG = high glucose; LV = low volume; HV = high volume. Experiments were repeated 3 times with cells isolated from different animals. Data are represented as mean ± SD. Statistically significant increase in ATP content compared to LV is denoted by *($p<0.05$), **($p<0.01$).

because of lower availability of ATP; however, differences in treatment of the samples for evaluation may also be responsible for this difference.

5.2 Levels of endogenous polyP in cartilage constructs

The molecule polyP has been observed in native articular cartilage, suggesting that it may be endogenously produced, and has been associated with bioenergetic functions in other tissues. Evaluating the levels of polyP in tissues may therefore be an important element of the evaluation of the bioenergetic state of the cells. In order to determine the impact culture conditions have on endogenous polyP levels, this biomolecule was characterized via quantification, imaging, and exopolyphosphatase activity. Quantification of levels illustrated in Figure 17A demonstrated significantly less polyP levels in the constructs grown in LG-LV media than constructs grown in LG-HV and HG-LV media harvested 48 hours after media change ($p<0.05$). These constructs with greater polyP levels likely have a higher energetic state which enables the production of increased tissue formation for these media conditions [86]. No major differences in levels of polyP at 6 hours after media change were reported between conditions. As well, each condition had comparable levels of polyP at 6 hours and 48 hours after media change. When normalized to wet weight, no significant differences in polyP content were reported for the different media conditions and harvesting time points (Figure 17B).

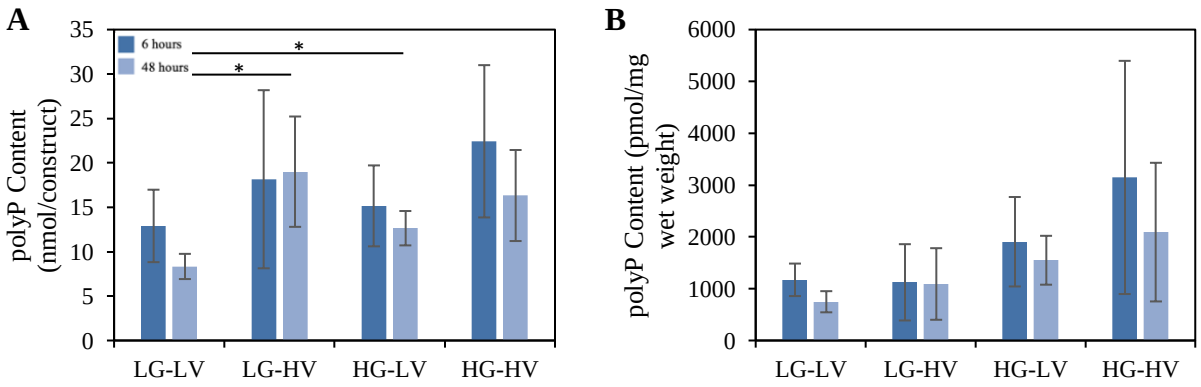

Figure 18. (A) Total polyP content in cartilage constructs and **(B)** normalized to wet weight on day 7 6 hours and 48 hours after media change. LG = low glucose; HG = high glucose; LV = low volume; HV = high volume. Data are represented as mean ± SD. Statistically significant increase in polyP content compared to LV is denoted by *($p<0.05$).

To visualize polyP in the tissue, histological sections of constructs harvested on day 28 were stained with DAPI (Figure 18A). A qualitative analysis of the different conditions observed a stronger signal in the superficial and deep zone of the tissue compared to the middle zone.

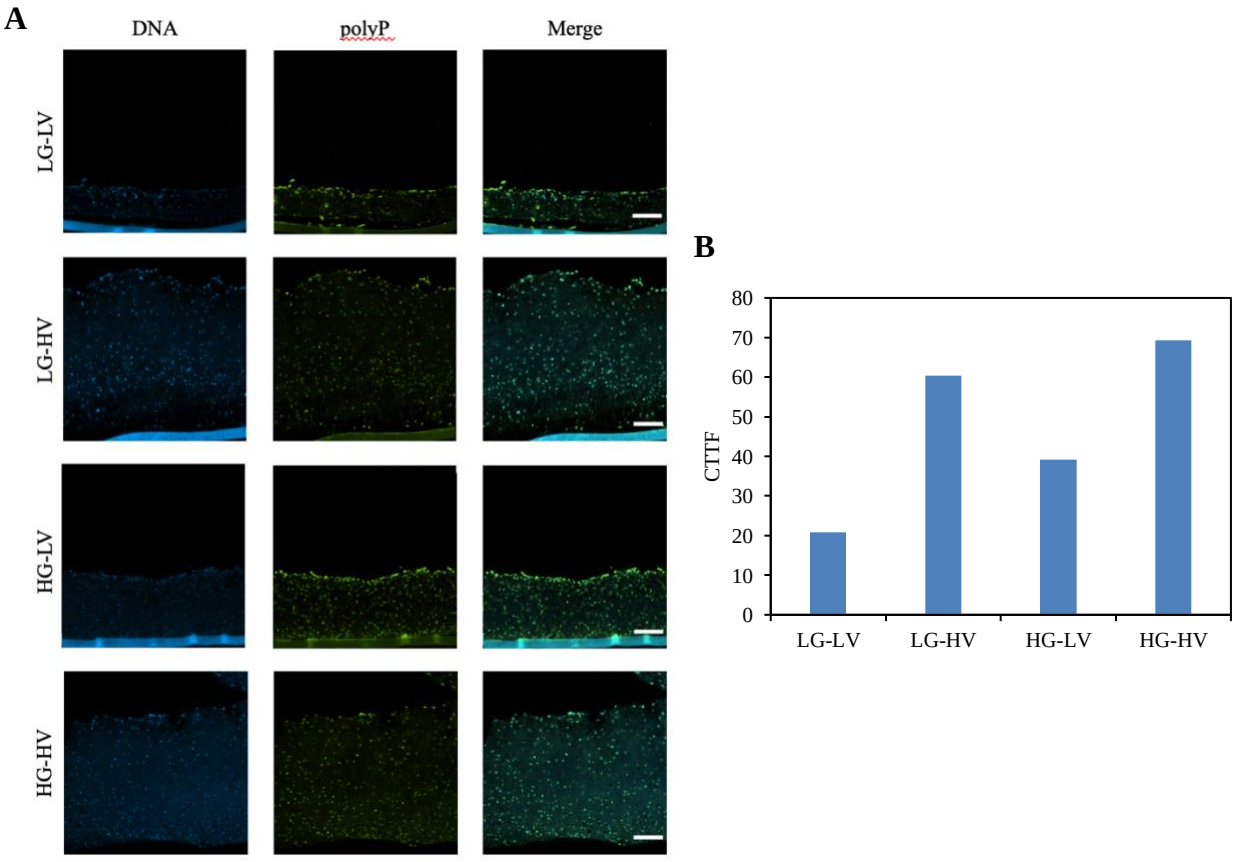

Figure 17. (A) Histological sections of each condition on day 28 stained with DAPI. Scale bar = 100 µm. **(B)** Quantification of fluorescence staining intensity. LG = low glucose; HG = high glucose; LV = low volume; HV = high volume. TCTF = total corrected tissue fluorescence. Data was collected from one replicate.

Notably, the HG-HV condition had less signal on the superficial zone compared to other conditions. Measurement of the integrated density of the images offered a quantitative analysis in which the trends for the different conditions correlated with those obtained from quantification methods of polyP (Figure 18B). However, repeated experiments are required in order to validate these results. The tissue grown in LG-HV media was digested with ALP to confirm that the signal represents the presence of polyP in the tissue. A decrease in signal after ALP digestion was observed and confirmed by measuring the integrated density of the image (Figure 19). However, some signal was still present particularly in areas that overlap with the presence of DNA. Three possibilities exist that may explain the remaining signal: (1) ALP may not have had access to all polyP in the tissue for digestion, whereby polyP tightly bound to other biomolecules may not be available for enzymatic hydrolysis, (2) the digestion protocol may require optimization e.g. longer incubation time, changes to incubation temperature, pH, or buffer composition, (3) unspecific binding of DAPI to other biomolecules could also result in misleading signal, for example overlap of emission spectra exists where DAPI bound to DNA leads to some fluorescence with the polyP filter which is hard to ascribe specifically to polyP in the nucleus versus DNA itself.

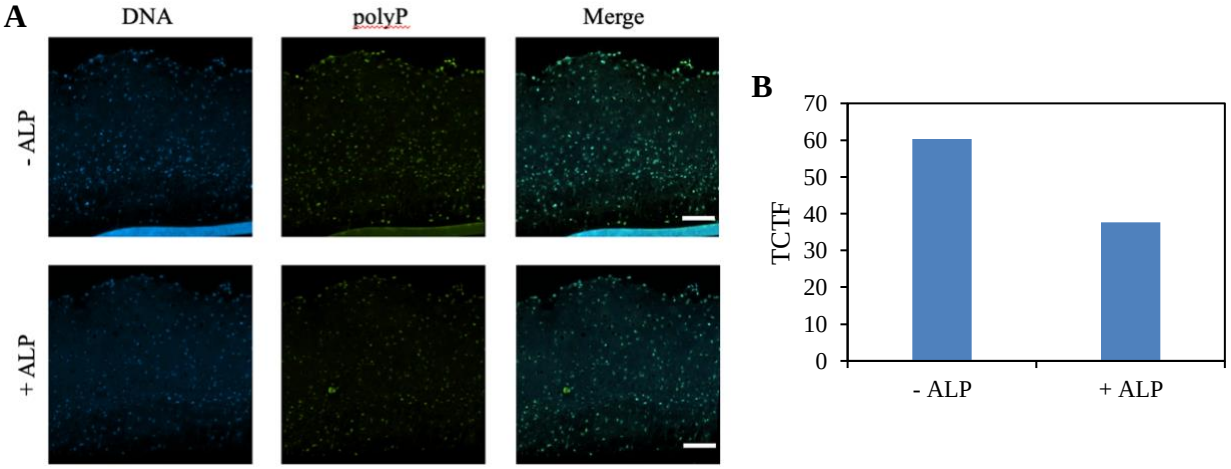

Figure 19. (A) Histological sections of LG-HV condition stained with DAPI either undigested with ALP (top) or digested with ALP (bottom). Scale bar = 100 µm. **(B)** Quantification of fluorescence staining intensity. TCTF = total corrected tissue fluorescence. Data was collected from one replicate.

Exopolyphosphatase activity is a parameter often measured in parallel to evaluation of polyP levels in the tissue. Exopolyphosphatases are enzymes that cleave phosphate groups off the end of the polyP polymer and therefore contributes to the catabolism of polyP. While the specific enzymes involved in this process are not fully elucidated, an assay that incubates tissue extracts with polyP and measures the quantity of phosphate produced provides insight on enzyme activity in the construct. Figure 20 illustrates the exopolyphosphatase activity from constructs harvested on day 7 6 hours after media change. Our results indicate a significantly higher activity in the HG-LV construct compared to the LG-HV construct ($p<0.05$). The action of exopolyphosphatases may limit the effect endogenous polyP has on the metabolic state of the tissue. The activity reported here is much smaller than previous studies [117] and, therefore, further work may be required to understand these differences.

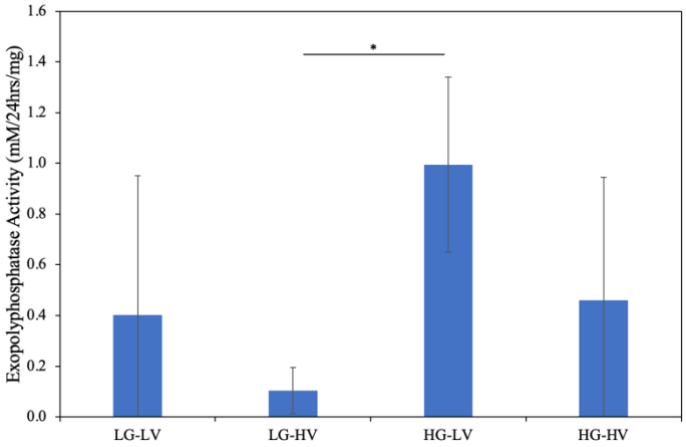

Figure 20. Exopolyphosphatase activity of cartilage constructs harvested on day 7 6 hours after media change. LG = low glucose; HG = high glucose; LV = low volume; HV = high volume. Data are represented as mean ± SD. Statistically significant increase in exopolyphosphatase activity compared to LG-HV is denoted by *($p<0.05$).

PolyP was also quantified in the media to determine whether polyP is synthesized and released from the constructs. Our results indicate similar amounts of polyP in the media with tissue as media without tissue (Figure 21). During the process of extracting polyP from the media, there may have been insufficient amounts of proteinase K available to digest all the protein in the media. Any endogenous exopolyphosphatases present in the media could have digested polyP and underestimate polyP levels potentially released by chondrocytes. However, we also speculate that the source of polyP in the media without tissue could come from FBS supplementation. This finding raises a key question as to the origin of the polyP in tissue constructs. In other words, it is unclear based on this result if chondrocytes can synthesize polyP endogenously or if polyP is available exogenously from the culture medium, or in the case of native tissues from the synovial fluid which is an ultrafiltrate of plasma. Future work is required to answer this important question.

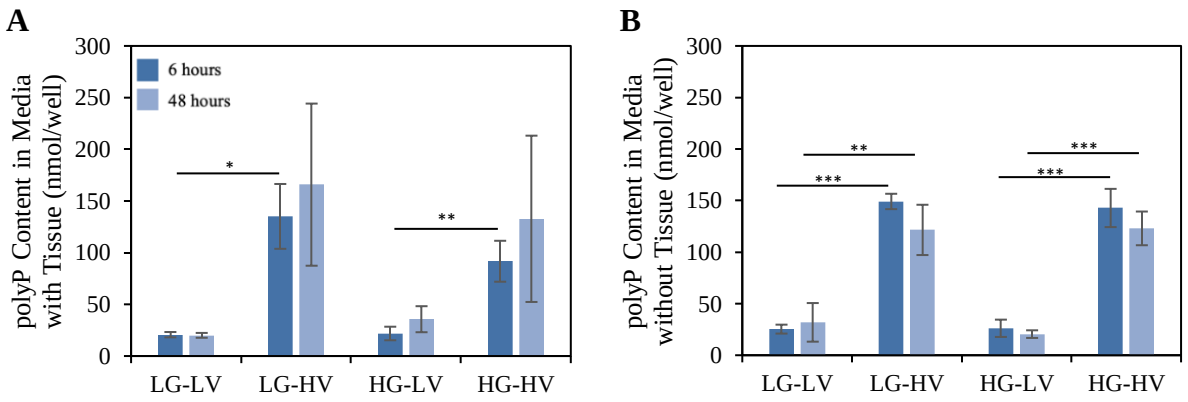

Figure 21. (A) Total polyP content in the media with cartilage constructs and **(B)** total polyP content in the media without cartilage constructs. LG = low glucose; HG = high glucose; LV = low volume; HV = high volume. Data are represented as mean ± SD. Statistically significant difference in polyP content is denoted by *($p<0.05$), **($p<0.01$), ***($p<0.001$).

5.3 Effect of pyruvate and glutamine on metabolic pathways

During this work, another student in the group obtained data to suggest that pyruvate and glutamate additions in the culture medium have a profound effect on ECM accumulation. In this work, as was stated previously, culture media had these additions. That preliminary study conducted in our group also suggested that the addition of exogenous polyP has differential effects on matrix accumulation in cartilage constructs cultured in media supplemented with different nutrients. Specifically, when pyruvate and glutamine are present in the media, as it is for this project, exogenous polyP had minimal effect on matrix accumulation, whereas an effect of polyP supplementation was measured in absence of these supplements. We speculated that the endogenous polyP levels in presence of the supplements may lead to high levels of polyP in the tissues such that addition of exogenous polyP may confer no additional benefit. Given our interest in evaluating if we can modulate polyP levels in tissues via culture conditions and because our results from modulating glucose levels and media volumes were relatively small, we wanted to test the effects of these additions on endogenous polyP levels to guide future work. Constructs were cultured for 7 days and harvested 48 hours after media change in media containing either pyruvate or glutamine, both pyruvate and glutamine, or without pyruvate and glutamine. Total polyP levels in the construct are illustrated in Figure 22A and demonstrate the highest levels when both pyruvate and glutamine were present in the media. If reproducible, these results would concur with our speculation that tissues cultured in supplemented media may already have saturating levels of endogenous polyP and the addition of exogenous polyP has little effect on matrix accumulation. When polyP is normalized to wet weight, there is a less noticeable difference in polyP levels between the different conditions (Figure 22B). Further insights may require

evaluating polyP levels in conjunction with DNA levels to gain information on the polyP levels per cell.

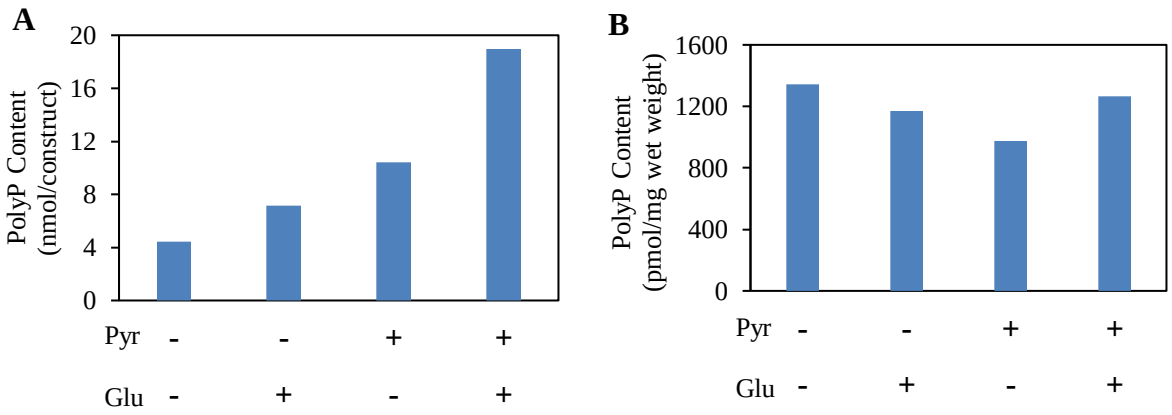

Figure 22. (A) Total polyP content in cartilage constructs and **(B)** normalized to wet weight harvested on day 7 48 hours after media change. Culture media was supplemented with (+) or without (-) pyruvate (Pyr) and/or glutamine (Glu). Data was collected from one biological replicate.

Total ATP content in the constructs is illustrated in Figure 23A and has the highest levels in the construct grown in media without pyruvate and glutamine. Similar trends are seen when normalized to wet weight (Figure 23B). Interestingly, Figure 24 suggests that the total amount of these bioenergetic molecules in the constructs are inversely correlated. This data provides interesting preliminary results regarding the impact different nutrients can have on the metabolic state of chondrocytes.

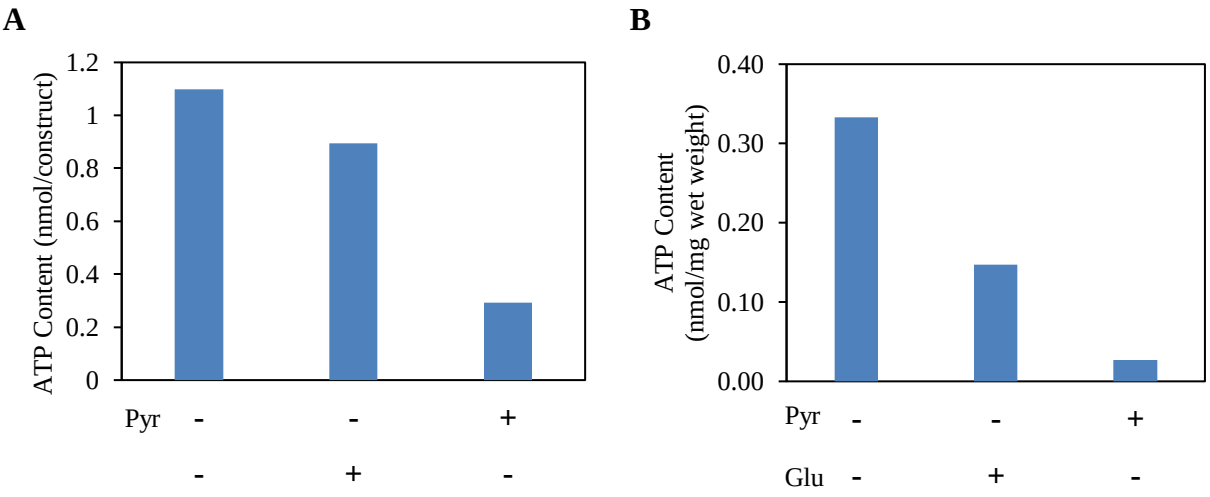

Figure 23. (A) Total ATP content in cartilage constructs and **(B)** normalized to wet weight on day 7 48 hours after media change. Culture media was supplemented with (+) or without (-) pyruvate (Pyr) and/or glutamine (Glu). Data was collected from one biological replicate.

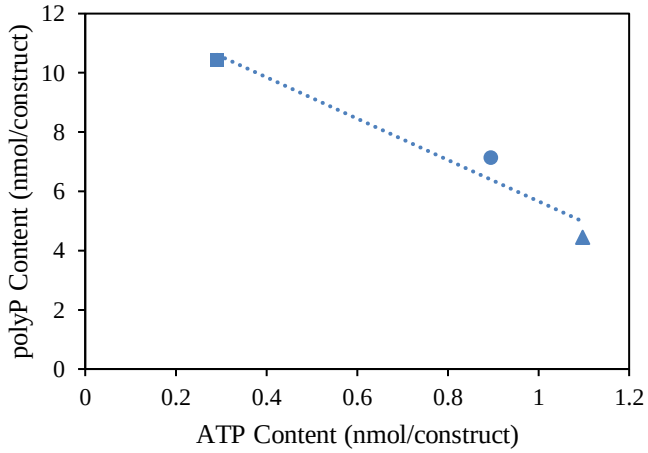

Figure 24. Correlation between polyP content and ATP content in tissues grown in LG-HV media without pyruvate and glutamine (▲), with only pyruvate (●), or with only glutamine (■). Data was collected from one biological replicate.

CONCLUDING STATEMENTS

6.1 Effect of glucose concentrations on cartilage constructs

Since glucose is the primary substrate of glycolysis and is a building block for proteoglycan synthesis, it has received plenty of attention when studying nutrient availability in cartilage constructs [20]–[22], [71]. For this project, we hypothesized that physiological glucose concentrations would be beneficial for tissue growth since supraphysiological glucose concentrations that are typically used for cartilage tissue culture have been shown to induce damaging chondrocyte responses [20], [21]. At low media volumes, the high glucose concentration generated constructs with increased collagen and sGAG content compared to the low glucose concentration. This may be explained by the depletion of glucose in the LG-LV media that occurred between media changes due to the batchwise nature of nutrient replenishment. However, at high media volumes, no major differences in cartilage composition between the different glucose concentrations were reported. These findings are supported by previous studies where glucose supplementation as an alternative method to increasing media volume did not significantly increase sGAG content in high media volumes, but did increase sGAG content in low media volumes [71].

Other scaffold-free systems also did not report differences in proteoglycan content when cultured in glucose concentrations ranging from 5-25 mM [20], [102]. As well, our results demonstrated a similar glucose consumption rate for the four conditions potentially owing to similar diffusion rates. Comparable glucose consumption rates, supported by similar levels of glucose uptake, may in turn lead to similar metabolic rates and biosynthesis of matrix components.

This offers a potential explanation as to why the low and high glucose concentrations accumulated similar levels of sGAG and collagen in high media volumes.

It should also be noted that although different glucose concentrations did not lead to differences in the quantified matrix levels, histological sections showed improved tissue structure identified by homogenous tissue with spherical chondrocytes. Physiological glucose concentrations may impact the assembly of proteoglycans into aggregates and cross-linking of the collagen fibers into a complex network. This notion is supported by a study where constructs exposed to deformational loading generated superior mechanical properties compared to free-swelling constructs despite both conditions having similar levels of matrix components [19]. The quantified levels of matrix components may not always correlate with the functional integrity of the tissue or, in our case, the morphology of the cells. These results suggest that more specific measurements may be required to identify differences in tissues cultured with different glucose concentrations. These will be discussed in future work.

6.2 Effect of media volume on cartilage constructs

Increasing the volume of media served as a method to prevent a depletion of glucose when the concentration was adjusted to similar conditions found within the joint. Greater media volumes enhanced the matrix accumulation at both physiological and supraphysiological glucose concentrations as seen in other studies [71], [102]. However, the precise mechanism to explain why increased volume is superior remains unclear. Some studies hypothesize that glucose is the limiting agent since its depletion may lead to impaired cell viability and cartilage formation [22]. This may provide an explanation for the LG-LV condition where glucose starvation occurred, but it does not explain why the HG-LV condition had significantly less matrix accumulation than the HG-HV condition despite having sufficient glucose in the media between media changes.

Increasing the medium volume increases the supply of multiple different nutrients including amino acids, serum-derived growth factors as well as glucose, which further supports the need to investigate the impact of other nutrients on cartilage formation. Alternatively, the accumulation of waste products in the low volumes, as seen in our results, may promote an acidic environment that can impact cell viability. The application of hydrostatic pressure has also demonstrated superior biomechanical and biochemical properties for cartilage constructs [12], however, hydrostatic pressure did not play a role in this study since the height of media for both volumes is the same in our system. The dissolution of oxygen may also play a role depending on the dimensions of a larger vessel because oxygen diffused through surface area but concentration is related to volume; however, it is unlikely an important factor for this project since the surface area to volume ratios were similar for the different media volumes. Identifying the key mechanism by which larger media volumes offer a benefit for cartilage tissue engineering in order to develop alternative strategies that provide the same benefits as larger media volumes without the accompanying costs and resources is crucial and will be pursued in future works.

6.3 Metabolic processes in cartilage constructs

The comparable consumption rate of the different conditions provides an explanation for the quantified matrix molecules. Overall trends for sGAG, collagen, and polyP content demonstrate a significant increase in the LG-HV condition compared to LG-LV, meanwhile the difference between the HG-LV and HG-HV conditions is minimized, and the values associated with these conditions are often similar to LG-HV values. If glucose is consumed at similar rates, all conditions are uptaking equivalent amounts of this bioenergetic molecule until it is depleted, as observed in the LG-LV condition. We wanted to further investigate the metabolic processes carried out in cartilage constructs by evaluating the relationships between lactate release and glucose uptake as

well as ATP and polyP production. The ratio of lactate released-to-glucose uptake may have been influenced by other nutrients in the media, including pyruvate and glutamine. Another study that used media without pyruvate and glutamine explained that the production of lactate accounted for most of the glucose uptake which is consistent with the anaerobic processes of native cartilage [71], [78]. We cannot yet conclude that this occurs in our system, but future work can reveal the complex relationships that exist between pyruvate, glutamine, lactate, and glucose. The relationship between polyP and ATP is also not clear in part due to the minimal research dedicated to polyP in mammalian tissues. Interestingly, our results indicate that there are greater molar levels of polyP than ATP in the tissues. A closer look at the LG-LV condition shows that ATP content increases between 6 and 48 hours meanwhile polyP content decreases. We speculate that polyP is being converted to ATP as a compensation method to maintain energy levels when there is a depletion of glucose and could therefore serve as a bioenergetic storage molecule [86]. Finally, preliminary data that evaluates the effect of pyruvate and glutamine in the media on cartilage constructs suggests that certain nutrients can impact neocartilage formation in different ways. The combination of different nutrients and environmental factors likely impact the complex metabolic processes conducted by chondrocytes and should continue to be investigated in order to identify optimal culture conditions that grow high-quality tissue-engineered cartilage constructs.

6.4 Future work

This thesis has provided a roadmap towards the approach selected in our group for optimizing the culture conditions of *in vitro* cartilage maturation. In the near future, next steps are required to provide a more complete picture of the impact of the two culture parameters investigated in this thesis. In order to develop a deeper understanding of the biochemical composition of the constructs, gene expression and immunohistochemistry studies should be conducted to determine

if glucose concentration and media volume impact the types of collagen in the tissue. It will also be critical to evaluate the source of polyP quantified in the tissues (endogenous production by chondrocytes or exogenous accumulation from the medium). To determine whether it is sourced in FBS, tissues should be cultured with ITS and/or with FBS in which polyP levels are reduced via enzymatic digestion followed by inactivation of the enzymes with heat. As well, repeats of DAPI staining on histology sections to localize polyP is required to confirm our findings. Future analysis of these histological images will include measuring the circularity of the chondrocytes in the tissue and quantifying the level of DAPI staining intensity through the depth of the tissue. We may also need to add replicates for specific experiments. Unfortunately, many of these experiments were cut short by supply chain issues, which interrupted access to cell culture inserts.

The culture system may also need to be modified in order to optimize a protocol for measuring the mechanical properties of the engineered constructs. The mechanical properties will need to be investigated to determine the functional nature of the constructs. These modifications may involve the deposition of a platen on the top surface of the tissue for specific periods every day to ensure the tissue grows with a flat surface. It is also important to determine the mechanical test that is most appropriate for our system.

Preliminary work in this project brought to light the possibility that other nutrients in the media may impact the metabolic processes and composition of the tissue. An initial experiment demonstrated that pyruvate and glutamine can impact the levels of metabolites produced in the tissues and this experiment must be repeated to validate these findings. Pertinent to this study, the tissue composition of cartilage constructs grown in different media should also be investigated.

Future work should also investigate the potential of providing a stable nutrient environment for the constructs. Increasing the media volume of physiological glucose concentrations

dramatically improved the stability of the nutrient environment and increased matrix accumulation of the constructs, yet the glucose concentration still decreased by 45.2±10.2% before the next media change. At high media volumes, the initial glucose content in HG is over 4 times greater than LG (49.5 mg glucose vs 11.0 mg, respectively). It may be interesting to investigate the stability of the nutrient environment if the volume of LG was adjusted to have the same initial glucose content as the HG-HV media. Having said that, further increasing the media volume can be costly and not feasible for a high throughput of experiments. An alternative strategy could involve the development of a continuous bioreactor as a mode of nutrient replenishment with an inlet that can continuously supply glucose in order to maintain constant glucose concentrations. Another strategy can explore culturing microconstructs which would require fewer primary chondrocytes and increase the yield of experiments that can be conducted simultaneously. To take on this strategy I worked with a collaborating institution in London (UK) where I learned how to combine 3D printed moulds and soft lithography to construct PDMS microconstructs. Biofunctionalization of these constructs, as described in the methods, needs to be tested and optimized to provide the best seeding conditions for chondrocyte attachment and cartilage formation.

REFERENCES

[1] P. H. A. of Canada, "Osteoarthritis in Canada," Sep. 29, 2020. https://www.canada.ca/en/public-health/services/publications/diseases-conditions/osteoarthritis.html (accessed Jul. 24, 2022).

[2] R. F. Loeser, S. R. Goldring, C. R. Scanzello, and M. B. Goldring, "Osteoarthritis: A Disease of the Joint as an Organ," *Arthritis Rheum*, vol. 64, no. 6, pp. 1697–1707, Jun. 2012, doi: 10.1002/art.34453.

[3] J. Eschweiler *et al.*, "The Biomechanics of Cartilage—An Overview," *Life*, vol. 11, no. 4, Art. no. 4, Apr. 2021, doi: 10.3390/life11040302.

[4] C. W. Archer and P. Francis-West, "The chondrocyte," *Int J Biochem Cell Biol*, vol. 35, no. 4, pp. 401–404, Apr. 2003, doi: 10.1016/s1357-2725(02)00301-1.

[5] E. B. Hunziker, "Articular cartilage repair: are the intrinsic biological constraints undermining this process insuperable?," *Osteoarthritis and Cartilage*, vol. 7, no. 1, pp. 15–28, Jan. 1999, doi: 10.1053/joca.1998.0159.

[6] "Articular Cartilage: Injuries and Potential for Healing." http://www.jospt.org/doi/epdf/10.2519/jospt.1998.28.4.192 (accessed Sep. 27, 2022).

[7] H. K. Kim, M. E. Moran, and R. B. Salter, "The potential for regeneration of articular cartilage in defects created by chondral shaving and subchondral abrasion. An experimental investigation in rabbits.," *JBJS*, vol. 73, no. 9, pp. 1301–1315, Oct. 1991.

[8] M. Khalid, S. Tufail, Z. Aslam, and A. Butt, "Osteoarthritis: From complications to cure," *International Journal of Clinical Rheumatology*, vol. 12, no. 6, p. 160, 2017, doi: 10.4172/1758-4272.1000152.

[9] E. A. Makris, A. H. Gomoll, K. N. Malizos, J. C. Hu, and K. A. Athanasiou, “Repair and tissue engineering techniques for articular cartilage,” *Nat Rev Rheumatol*, vol. 11, no. 1, pp. 21–34, Jan. 2015, doi: 10.1038/nrrheum.2014.157.

[10] A. Getgood, R. Brooks, L. Fortier, and N. Rushton, “Articular cartilage tissue engineering,” *The Journal of Bone and Joint Surgery. British volume*, vol. 91-B, no. 5, pp. 565–576, May 2009, doi: 10.1302/0301-620X.91B5.21832.

[11] J.-L. Chen, L. Duan, W. Zhu, J. Xiong, and D. Wang, “Extracellular matrix production in vitro in cartilage tissue engineering,” *J Transl Med*, vol. 12, no. 1, Art. no. 1, Dec. 2014, doi: 10.1186/1479-5876-12-88.

[12] B. D. Elder and K. A. Athanasiou, “Synergistic and Additive Effects of Hydrostatic Pressure and Growth Factors on Tissue Formation,” *PLOS ONE*, vol. 3, no. 6, p. e2341, Jun. 2008, doi: 10.1371/journal.pone.0002341.

[13] U. Hansen *et al.*, “Combination of reduced oxygen tension and intermittent hydrostatic pressure: a useful tool in articular cartilage tissue engineering,” *Journal of Biomechanics*, vol. 34, no. 7, pp. 941–949, Jul. 2001, doi: 10.1016/S0021-9290(01)00050-1.

[14] J. Lam, S. Lu, F. K. Kasper, and A. G. Mikos, “Strategies for controlled delivery of biologics for cartilage repair,” *Advanced Drug Delivery Reviews*, vol. 84, pp. 123–134, Apr. 2015, doi: 10.1016/j.addr.2014.06.006.

[15] R. L. Mauck, S. L. Seyhan, G. A. Ateshian, and C. T. Hung, “Influence of Seeding Density and Dynamic Deformational Loading on the Developing Structure/Function Relationships of Chondrocyte-Seeded Agarose Hydrogels,” *Annals of Biomedical Engineering*, vol. 30, no. 8, pp. 1046–1056, Sep. 2002, doi: 10.1114/1.1512676.

[16] C. Mennan *et al.*, "Human Articular Chondrocytes Retain Their Phenotype in Sustained Hypoxia While Normoxia Promotes Their Immunomodulatory Potential," *CARTILAGE*, vol. 10, no. 4, pp. 467–479, Oct. 2019, doi: 10.1177/1947603518769714.

[17] S. Razaq, R. J. Wilkins, and J. P. G. Urban, "The effect of extracellular pH on matrix turnover by cells of the bovine nucleus pulposus," *Eur Spine J*, vol. 12, no. 4, pp. 341–349, Aug. 2003, doi: 10.1007/s00586-003-0582-3.

[18] R. A. J. Windhaber, R. J. Wilkins, and D. Meredith, "Functional characterisation of glucose transport in bovine articular chondrocytes," *Pflugers Arch - Eur J Physiol*, vol. 446, no. 5, pp. 572–577, Aug. 2003, doi: 10.1007/s00424-003-1080-5.

[19] R. L. Mauck, C. C.-B. Wang, E. S. Oswald, G. A. Ateshian, and C. T. Hung, "The role of cell seeding density and nutrient supply for articular cartilage tissue engineering with deformational loading," *Osteoarthritis and Cartilage*, vol. 11, no. 12, pp. 879–890, Dec. 2003, doi: 10.1016/j.joca.2003.08.006.

[20] K. M. Kelley, T. R. Johnson, J. Ilan, and R. W. Moskowitz, "Glucose regulation of the IGF response system in chondrocytes: induction of an IGF-I-resistant state," *American Journal of Physiology-Regulatory, Integrative and Comparative Physiology*, vol. 276, no. 4, pp. R1164–R1171, Apr. 1999, doi: 10.1152/ajpregu.1999.276.4.R1164.

[21] S. C. Rosa, A. T. Rufino, F. M. Judas, C. M. Tenreiro, M. C. Lopes, and A. F. Mendes, "Role of glucose as a modulator of anabolic and catabolic gene expression in normal and osteoarthritic human chondrocytes," *Journal of Cellular Biochemistry*, vol. 112, no. 10, pp. 2813–2824, 2011, doi: 10.1002/jcb.23196.

[22] H. K. Heywood, P. K. Sembi, D. A. Lee, and D. L. Bader, "Cellular Utilization Determines Viability and Matrix Distribution Profiles in Chondrocyte-Seeded Alginate Constructs,"

Tissue Engineering, vol. 10, no. 9–10, pp. 1467–1479, Sep. 2004, doi: 10.1089/ten.2004.10.1467.

[23] M. R. W. Brown and A. Kornberg, "Inorganic polyphosphate in the origin and survival of species," *Proceedings of the National Academy of Sciences*, vol. 101, no. 46, pp. 16085–16087, Nov. 2004, doi: 10.1073/pnas.0406909101.

[24] A. Kornberg, N. N. Rao, and D. Ault-Riché, "Inorganic Polyphosphate: A Molecule of Many Functions," *Annu. Rev. Biochem.*, vol. 68, no. 1, pp. 89–125, Jun. 1999, doi: 10.1146/annurev.biochem.68.1.89.

[25] K. D. Kumble and A. Kornberg, "Inorganic Polyphosphate in Mammalian Cells and Tissues," *Journal of Biological Chemistry*, vol. 270, no. 11, pp. 5818–5822, Mar. 1995, doi: 10.1074/jbc.270.11.5818.

[26] J.-P. St-Pierre *et al.*, "Inorganic polyphosphate exhibits anabolic effects on articular cartilage," *Osteoarthritis and Cartilage*, vol. 20, p. S39, Apr. 2012, doi: 10.1016/j.joca.2012.02.572.

[27] V. C. Mow, A. Ratcliffe, and A. Robin Poole, "Cartilage and diarthrodial joints as paradigms for hierarchical materials and structures," *Biomaterials*, vol. 13, no. 2, pp. 67–97, Jan. 1992, doi: 10.1016/0142-9612(92)90001-5.

[28] J. M. Mansour, "Biomechanics of Cartilage," p. 14.

[29] A. J. Sophia Fox, A. Bedi, and S. A. Rodeo, "The Basic Science of Articular Cartilage: Structure, Composition, and Function," *Sports Health*, vol. 1, no. 6, pp. 461–468, Nov. 2009, doi: 10.1177/1941738109350438.

[30] C. A. Poole, M. H. Flint, and B. W. Beaumont, “Chondrons in cartilage: ultrastructural analysis of the pericellular microenvironment in adult human articular cartilages,” *J Orthop Res*, vol. 5, no. 4, pp. 509–522, 1987, doi: 10.1002/jor.1100050406.

[31] A. R. Poole, T. Kojima, T. Yasuda, F. Mwale, M. Kobayashi, and S. Laverty, “Composition and Structure of Articular Cartilage: A Template for Tissue Repair,” *Clinical Orthopaedics and Related Research®*, vol. 391, p. S26, Oct. 2001.

[32] L. J. Sandell and T. Aigner, “Articular cartilage and changes in Arthritis: Cell biology of osteoarthritis,” *Arthritis Research & Therapy*, vol. 3, no. 2, p. 107, Jan. 2001, doi: 10.1186/ar148.

[33] D. H. Vynios, “Metabolism of Cartilage Proteoglycans in Health and Disease,” *Biomed Res Int*, vol. 2014, p. 452315, 2014, doi: 10.1155/2014/452315.

[34] T. Walimbe and A. Panitch, “Proteoglycans in Biomedicine: Resurgence of an Underexploited Class of ECM Molecules,” *Frontiers in Pharmacology*, vol. 10, p. 1661, 2020, doi: 10.3389/fphar.2019.01661.

[35] D. Eyre, “Articular cartilage and changes in Arthritis: Collagen of articular cartilage,” *Arthritis Res*, vol. 4, no. 1, pp. 30–35, 2002, doi: 10.1186/ar380.

[36] M. A. Cremer, E. F. Rosloniec, and A. H. Kang, “The cartilage collagens: a review of their structure, organization, and role in the pathogenesis of experimental arthritis in animals and in human rheumatic disease,” *Journal of Molecular Medicine*, vol. 76, no. 3–4, pp. 275–288, Feb. 1998, doi: 10.1007/s001090050217.

[37] D. Martínez-Moreno, G. Jiménez, P. Gálvez-Martín, G. Rus, and J. A. Marchal, “Cartilage biomechanics: A key factor for osteoarthritis regenerative medicine,” *Biochimica et*

Biophysica Acta (BBA) - Molecular Basis of Disease, vol. 1865, no. 6, pp. 1067–1075, Jun. 2019, doi: 10.1016/j.bbadis.2019.03.011.

[38] N. A. Zelenski *et al.*, "Collagen VI regulates pericellular matrix properties, chondrocyte swelling, and mechanotransduction in articular cartilage," *Arthritis Rheumatol*, vol. 67, no. 5, pp. 1286–1294, May 2015, doi: 10.1002/art.39034.

[39] T. Kirsch and K. von der Mark, "Remodelling of collagen types I, II and X and calcification of human fetal cartilage," *Bone and Mineral*, vol. 18, no. 2, pp. 107–117, Aug. 1992, doi: 10.1016/0169-6009(92)90851-4.

[40] "The Donnan model derived from microstructure," *Biophysical Chemistry*, vol. 46, no. 1, pp. 57–68, Feb. 1993, doi: 10.1016/0301-4622(93)87007-J.

[41] R. K. Korhonen, P. Julkunen, W. Wilson, and W. Herzog, "Importance of Collagen Orientation and Depth-Dependent Fixed Charge Densities of Cartilage on Mechanical Behavior of Chondrocytes," *Journal of Biomechanical Engineering*, vol. 130, no. 2, Mar. 2008, doi: 10.1115/1.2898725.

[42] P. N. Bansal, N. S. Joshi, V. Entezari, M. W. Grinstaff, and B. D. Snyder, "Contrast Enhanced Computed Tomography can predict the glycosaminoglycan content and biomechanical properties of articular cartilage," *Osteoarthritis and Cartilage*, vol. 18, no. 2, pp. 184–191, Feb. 2010, doi: 10.1016/j.joca.2009.09.003.

[43] Z. Zhang, "Chondrons and the Pericellular Matrix of Chondrocytes," *Tissue Engineering Part B: Reviews*, vol. 21, no. 3, pp. 267–277, Jun. 2015, doi: 10.1089/ten.teb.2014.0286.

[44] P. S. Eggli, W. Herrmann, E. B. Hunziker, and R. K. Schenk, "Matrix compartments in the growth plate of the proximal tibia of rats," *The Anatomical Record*, vol. 211, no. 3, pp. 246–257, 1985, doi: 10.1002/ar.1092110304.

[45] S. Glyn-Jones *et al.*, "Osteoarthritis," *The Lancet*, vol. 386, no. 9991, pp. 376–387, Jul. 2015, doi: 10.1016/S0140-6736(14)60802-3.

[46] N. Arden and M. C. Nevitt, "Osteoarthritis: Epidemiology," *Best Practice & Research Clinical Rheumatology*, vol. 20, no. 1, pp. 3–25, Feb. 2006, doi: 10.1016/j.berh.2005.09.007.

[47] R. F. Loeser, "Molecular mechanisms of cartilage destruction in osteoarthritis," p. 4.

[48] M. B. Mueller and R. S. Tuan, "Anabolic/Catabolic Balance in Pathogenesis of Osteoarthritis: Identifying Molecular Targets," *PM&R*, vol. 3, no. 6S, pp. S3–S11, 2011, doi: 10.1016/j.pmrj.2011.05.009.

[49] G. Man and G. Mologhianu, "Osteoarthritis pathogenesis – a complex process that involves the entire joint," *J Med Life*, vol. 7, no. 1, pp. 37–41, Mar. 2014.

[50] L. A. Setton, D. M. Elliott, and V. C. Mow, "Altered mechanics of cartilage with osteoarthritis: human osteoarthritis and an experimental model of joint degeneration," *Osteoarthritis and Cartilage*, vol. 7, no. 1, pp. 2–14, Jan. 1999, doi: 10.1053/joca.1998.0170.

[51] K. D. Allen, S. B. Adams, and L. A. Setton, "Evaluating Intra-Articular Drug Delivery for the Treatment of Osteoarthritis in a Rat Model," *Tissue Engineering Part B: Reviews*, vol. 16, no. 1, pp. 81–92, Feb. 2010, doi: 10.1089/ten.teb.2009.0447.

[52] C. B. Little and D. J. Hunter, "Post-traumatic osteoarthritis: from mouse models to clinical trials," *Nat Rev Rheumatol*, vol. 9, no. 8, Art. no. 8, Aug. 2013, doi: 10.1038/nrrheum.2013.72.

[53] R. Vaishya, G. B. Pariyo, A. K. Agarwal, and V. Vijay, “Non-operative management of osteoarthritis of the knee joint,” *Journal of Clinical Orthopaedics and Trauma*, vol. 7, no. 3, pp. 170–176, Jul. 2016, doi: 10.1016/j.jcot.2016.05.005.

[54] K. Raja and N. Dewan, “Efficacy of Knee Braces and Foot Orthoses in Conservative Management of Knee Osteoarthritis: A Systematic Review,” *American Journal of Physical Medicine & Rehabilitation*, vol. 90, no. 3, pp. 247–262, Mar. 2011, doi: 10.1097/PHM.0b013e318206386b.

[55] H. A. Wieland, M. Michaelis, B. J. Kirschbaum, and K. A. Rudolphi, “Osteoarthritis — an untreatable disease?,” *Nat Rev Drug Discov*, vol. 4, no. 4, pp. 331–344, Apr. 2005, doi: 10.1038/nrd1693.

[56] J. Lützner, P. Kasten, K.-P. Günther, and S. Kirschner, “Surgical options for patients with osteoarthritis of the knee,” *Nat Rev Rheumatol*, vol. 5, no. 6, Art. no. 6, Jun. 2009, doi: 10.1038/nrrheum.2009.88.

[57] M. Brittberg, “Autologous chondrocyte implantation—Technique and long-term follow-up,” *Injury*, vol. 39, no. 1, Supplement, pp. 40–49, Apr. 2008, doi: 10.1016/j.injury.2008.01.040.

[58] M. Krill, N. Early, J. S. Everhart, and D. C. Flanigan, “Autologous Chondrocyte Implantation (ACI) for Knee Cartilage Defects: A Review of Indications, Technique, and Outcomes,” *JBJS Reviews*, vol. 6, no. 2, p. e5, Feb. 2018, doi: 10.2106/JBJS.RVW.17.00078.

[59] L. Duan *et al.*, “Cytokine networking of chondrocyte dedifferentiation in vitro and its implications for cell-based cartilage therapy,” *Am J Transl Res*, vol. 7, no. 2, pp. 194–208, Feb. 2015.

[60] D. Pape, G. Filardo, E. Kon, C. N. van Dijk, and H. Madry, “Disease-specific clinical problems associated with the subchondral bone,” *Knee Surg Sports Traumatol Arthrosc*, vol. 18, no. 4, pp. 448–462, Apr. 2010, doi: 10.1007/s00167-010-1052-1.

[61] J. N. Katz, “Total joint replacement in osteoarthritis,” *Best Practice & Research Clinical Rheumatology*, vol. 20, no. 1, pp. 145–153, Feb. 2006, doi: 10.1016/j.berh.2005.09.003.

[62] K. Sinusas, “Osteoarthritis: diagnosis and treatment,” *Am Fam Physician*, vol. 85, no. 1, pp. 49–56, Jan. 2012.

[63] B. J. Huang, J. C. Hu, and K. A. Athanasiou, “Cell-based tissue engineering strategies used in the clinical repair of articular cartilage,” *Biomaterials*, vol. 98, pp. 1–22, Aug. 2016, doi: 10.1016/j.biomaterials.2016.04.018.

[64] J. M. Brenner *et al.*, “Implantation of Scaffold-Free Engineered Cartilage Constructs in a Rabbit Model for Chondral Resurfacing,” *Artificial Organs*, vol. 38, no. 2, pp. E21–E32, 2014, doi: 10.1111/aor.12199.

[65] C. Z. Jin *et al.*, “The Maturity of Tissue-Engineered Cartilage In Vitro Affects the Repairability for Osteochondral Defect,” *Tissue Eng Part A*, vol. 17, no. 23–24, pp. 3057–3065, Dec. 2011, doi: 10.1089/ten.tea.2010.0605.

[66] M. D. Buschmann, Y. A. Gluzband, A. J. Grodzinsky, and E. B. Hunziker, “Mechanical compression modulates matrix biosynthesis in chondrocyte/agarose culture,” p. 12.

[67] D. A. Lee and D. L. Bader, “Compressive strains at physiological frequencies influence the metabolism of chondrocytes seeded in agarose,” *J Orthop Res*, vol. 15, no. 2, pp. 181–188, Mar. 1997, doi: 10.1002/jor.1100150205.

[68] S. D. Waldman, C. G. Spiteri, M. D. Grynpas, R. M. Pilliar, J. Hong, and R. A. Kandel, “Effect of biomechanical conditioning on cartilaginous tissue formation in vitro,” *J Bone*

Joint Surg Am, vol. 85-A Suppl 2, pp. 101–105, 2003, doi: 10.2106/00004623-200300002-00013.

[69] S. D. Waldman, D. C. Couto, M. D. Grynpas, R. M. Pilliar, and R. A. Kandel, "A single application of cyclic loading can accelerate matrix deposition and enhance the properties of tissue-engineered cartilage," *Osteoarthritis and Cartilage*, vol. 14, no. 4, pp. 323–330, Apr. 2006, doi: 10.1016/j.joca.2005.10.007.

[70] S. Nagel-Heyer, C. Goepfert, P. Adamietz, N. M. Meenen, and R. Pörtner, "Cultivation of three-dimensional cartilage-carrier-constructs under reduced oxygen tension," *Journal of Biotechnology*, vol. 121, no. 4, pp. 486–497, Feb. 2006, doi: 10.1016/j.jbiotec.2005.07.026.

[71] "Glucose Concentration and Medium Volume Influence Cell Viability and Glycosaminoglycan Synthesis in Chondrocyte-Seeded Alginate Constructs." https://www.liebertpub.com/doi/epdf/10.1089/ten.2006.12.3487 (accessed Feb. 23, 2022).

[72] "Glucose transport and metabolism in chondrocytes: a key to understanding chondrogenesis, skeletal development and cartilage degradation in osteoarthritis," *Histology and Histopathology*, no. 17, pp. 1239–1267, Oct. 2002, doi: 10.14670/HH-17.1239.

[73] R. B. Lee, R. J. Wilkins, S. Razaq, and J. P. G. Urban, "energy metabolism."

[74] S. Richardson *et al.*, "Molecular characterization and partial cDNA cloning of facilitative glucose transporters expressed in human articular chondrocytes; stimulation of 2-deoxyglucose uptake by IGF-I and elevated MMP-2 secretion by glucose deprivation," *Osteoarthritis Cartilage*, vol. 11, no. 2, pp. 92–101, Feb. 2003, doi: 10.1053/joca.2002.0858.

[75] J. M. Hollander and L. Zeng, “The Emerging Role of Glucose Metabolism in Cartilage Development,” *Curr Osteoporos Rep*, vol. 17, no. 2, pp. 59–69, Apr. 2019, doi: 10.1007/s11914-019-00506-0.

[76] J. A. Collins, R. J. Moots, R. Winstanley, P. D. Clegg, and P. I. Milner, “Oxygen and pH-sensitivity of human osteoarthritic chondrocytes in 3-D alginate bead culture system,” *Osteoarthritis Cartilage*, vol. 21, no. 11, pp. 1790–1798, Nov. 2013, doi: 10.1016/j.joca.2013.06.028.

[77] R. J. Wilkins and A. C. Hall, “Control of matrix synthesis in isolated bovine chondrocytes by extracellular and intracellular pH,” *Journal of Cellular Physiology*, vol. 164, no. 3, pp. 474–481, 1995, doi: 10.1002/jcp.1041640305.

[78] R. B. Lee and J. P. Urban, “Evidence for a negative Pasteur effect in articular cartilage.,” *Biochem J*, vol. 321, no. Pt 1, pp. 95–102, Jan. 1997.

[79] M. S. Baker, J. Feigan, and D. A. Lowther, “The mechanism of chondrocyte hydrogen peroxide damage. Depletion of intracellular ATP due to suppression of glycolysis caused by oxidation of glyceraldehyde-3-phosphate dehydrogenase,” *J Rheumatol*, vol. 16, no. 1, pp. 7–14, Jan. 1989.

[80] C. Corciulo *et al.*, “Endogenous adenosine maintains cartilage homeostasis and exogenous adenosine inhibits osteoarthritis progression,” *Nat Commun*, vol. 8, no. 1, Art. no. 1, May 2017, doi: 10.1038/ncomms15019.

[81] B. McIntyre and M. E. Solesio, “Mitochondrial inorganic polyphosphate (polyP): the missing link of mammalian bioenergetics,” *Neural Regen Res*, vol. 16, no. 11, pp. 2227–2228, Mar. 2021, doi: 10.4103/1673-5374.310687.

[82] N. N. Rao, M. R. Gómez-García, and A. Kornberg, “Inorganic Polyphosphate: Essential for Growth and Survival,” *Annu. Rev. Biochem.*, vol. 78, no. 1, pp. 605–647, Jun. 2009, doi: 10.1146/annurev.biochem.77.083007.093039.

[83] F. Müller *et al.*, “Platelet Polyphosphates Are Proinflammatory and Procoagulant Mediators In Vivo,” *Cell*, vol. 139, no. 6, pp. 1143–1156, Dec. 2009, doi: 10.1016/j.cell.2009.11.001.

[84] D. Morimoto *et al.*, “Inorganic polyphosphate differentiates human mesenchymal stem cells into osteoblastic cells,” *J Bone Miner Metab*, vol. 28, no. 4, pp. 418–423, Jul. 2010, doi: 10.1007/s00774-010-0157-4.

[85] E. Zakharian, B. Thyagarajan, R. J. French, E. Pavlov, and T. Rohacs, “Inorganic Polyphosphate Modulates TRPM8 Channels,” *PLOS ONE*, vol. 4, no. 4, p. e5404, Apr. 2009, doi: 10.1371/journal.pone.0005404.

[86] E. Pavlov, R. Aschar-Sobbi, M. Campanella, R. J. Turner, M. R. Gómez-García, and A. Y. Abramov, “Inorganic Polyphosphate and Energy Metabolism in Mammalian Cells,” *J Biol Chem*, vol. 285, no. 13, pp. 9420–9428, Mar. 2010, doi: 10.1074/jbc.M109.013011.

[87] A. Y. Baev, P. R. Angelova, and A. Y. Abramov, “Inorganic polyphosphate is produced and hydrolyzed in F0F1-ATP synthase of mammalian mitochondria,” *Biochem J*, vol. 477, no. 8, pp. 1515–1524, Apr. 2020, doi: 10.1042/BCJ20200042.

[88] L. K. Seidlmayer, L. A. Blatter, E. Pavlov, and E. N. Dedkova, “Inorganic polyphosphate–an unusual suspect of the mitochondrial permeability transition mystery,” *Channels (Austin)*, vol. 6, no. 6, pp. 463–467, Nov. 2012, doi: 10.4161/chan.21939.

[89] M. E. Solesio, L. C. Garcia del Molino, P. A. Elustondo, C. Diao, J. C. Chang, and E. V. Pavlov, “Inorganic Polyphosphate is Required for Sustained Free Mitochondrial Calcium

Elevation, Following Calcium Uptake," *Cell Calcium*, vol. 86, p. 102127, Mar. 2020, doi: 10.1016/j.ceca.2019.102127.

[90] J.-P. St-Pierre, Q. Wang, S. Q. Li, R. M. Pilliar, and R. A. Kandel, "Inorganic polyphosphate stimulates cartilage tissue formation," *Tissue Eng Part A*, vol. 18, no. 11–12, pp. 1282–1292, Jun. 2012, doi: 10.1089/ten.TEA.2011.0356.

[91] T. Shiba *et al.*, "Modulation of Mitogenic Activity of Fibroblast Growth Factors by Inorganic Polyphosphate*," *Journal of Biological Chemistry*, vol. 278, no. 29, pp. 26788–26792, Jul. 2003, doi: 10.1074/jbc.M303468200.

[92] L. Wang, C. D. Fraley, J. Faridi, A. Kornberg, and R. A. Roth, "Inorganic polyphosphate stimulates mammalian TOR, a kinase involved in the proliferation of mammary cancer cells," *Proceedings of the National Academy of Sciences*, vol. 100, no. 20, pp. 11249–11254, Sep. 2003, doi: 10.1073/pnas.1534805100.

[93] R. Dreier, "Hypertrophic differentiation of chondrocytes in osteoarthritis: the developmental aspect of degenerative joint disorders," *Arthritis Res Ther*, vol. 12, no. 5, p. 216, 2010, doi: 10.1186/ar3117.

[94] X. Wang *et al.*, "Inorganic polyphosphates stimulates matrix production in human annulus fibrosus cells," *JOR Spine*, vol. 4, no. 2, Jun. 2021, doi: 10.1002/jsp2.1143.

[95] J. J. Christ, S. Willbold, and L. M. Blank, "Methods for the Analysis of Polyphosphate in the Life Sciences," *Anal. Chem.*, vol. 92, no. 6, pp. 4167–4176, Mar. 2020, doi: 10.1021/acs.analchem.9b05144.

[96] W. D. Lee, R. Gawri, T. Shiba, A.-R. Ji, W. L. Stanford, and R. A. Kandel, "Simple Silica Column–Based Method to Quantify Inorganic Polyphosphates in Cartilage and Other

Tissues," *CARTILAGE*, vol. 9, no. 4, pp. 417–427, Oct. 2018, doi: 10.1177/1947603517690856.

[97] R. Aschar-Sobbi *et al.*, "High Sensitivity, Quantitative Measurements of Polyphosphate Using a New DAPI-Based Approach," *J Fluoresc*, vol. 18, no. 5, pp. 859–866, Sep. 2008, doi: 10.1007/s10895-008-0315-4.

[98] P. R. Angelova *et al.*, "*In Situ* Investigation of Mammalian Inorganic Polyphosphate Localization Using Novel Selective Fluorescent Probes JC-D7 and JC-D8," *ACS Chem. Biol.*, vol. 9, no. 9, pp. 2101–2110, Sep. 2014, doi: 10.1021/cb5000696.

[99] S. A. Smith, Y. Wang, and J. H. Morrissey, "DNA ladders can be used to size polyphosphate resolved by polyacrylamide gel electrophoresis," *ELECTROPHORESIS*, vol. 39, no. 19, pp. 2454–2459, 2018, doi: 10.1002/elps.201800227.

[100] R. L. Goldberg and L. M. Kolibas, "An Improved Method for Determining Proteoglycans Synthesized by Chondrocytes in Culture," *Connective Tissue Research*, vol. 24, no. 3–4, pp. 265–275, Jan. 1990, doi: 10.3109/03008209009152154.

[101] R. A. Berg, "[17] Determination of 3- and 4-hydroxyproline," in *Methods in Enzymology*, vol. 82, Elsevier, 1982, pp. 372–398. doi: 10.1016/0076-6879(82)82074-0.

[102] J. M. T. Suits, A. A. Khan, and S. D. Waldman, "Glycogen storage in tissue-engineered cartilage," *Journal of Tissue Engineering and Regenerative Medicine*, vol. 2, no. 6, pp. 340–346, 2008, doi: 10.1002/term.102.

[103] A. G. Gouldin and J. L. Puetzer, "An Inducible Model for Unraveling the Effects of Advanced Glycation End-Products in Collagen with Age and Diabetes." bioRxiv, p. 2020.09.04.283473, Sep. 04, 2020. doi: 10.1101/2020.09.04.283473.

[104] W. C. Hayes, L. M. Keer, G. Herrmann, and L. F. Mockros, “A mathematical analysis for indentation tests of articular cartilage,” *Journal of Biomechanics*, vol. 5, no. 5, pp. 541–551, Sep. 1972, doi: 10.1016/0021-9290(72)90010-3.

[105] Y.-S. Cheng *et al.*, “PPP2R5C Couples Hepatic Glucose and Lipid Homeostasis,” *PLoS Genet*, vol. 11, no. 10, p. e1005561, Oct. 2015, doi: 10.1371/journal.pgen.1005561.

[106] J. A. Long and H. D. Guthrie, “Validation of a rapid, large-scale assay to quantify ATP concentration in spermatozoa,” *Theriogenology*, vol. 65, no. 8, pp. 1620–1630, May 2006, doi: 10.1016/j.theriogenology.2005.06.020.

[107] R. A. McCloy, S. Rogers, C. E. Caldon, T. Lorca, A. Castro, and A. Burgess, “Partial inhibition of Cdk1 in G2 phase overrides the SAC and decouples mitotic events,” *Cell Cycle*, vol. 13, no. 9, pp. 1400–1412, May 2014, doi: 10.4161/cc.28401.

[108] A. Bajic, R. Tarantino, L. L. Y. Chiu, T. Duever, and S. D. Waldman, “Optimization of culture media to enhance the growth of tissue engineered cartilage,” *Biotechnology Progress*, vol. 36, no. 5, p. e3017, Sep. 2020, doi: 10.1002/btpr.3017.

[109] A. K. Williamson, A. C. Chen, and R. L. Sah, “Compressive properties and function-composition relationships of developing bovine articular cartilage,” *J Orthop Res*, vol. 19, no. 6, pp. 1113–1121, Nov. 2001, doi: 10.1016/S0736-0266(01)00052-3.

[110] R. Marks, “Osteoarthritis and Articular Cartilage: Biomechanics and Novel Treatment Paradigms,” *AAR*, vol. 03, no. 04, pp. 297–309, 2014, doi: 10.4236/aar.2014.34039.

[111] A. J. Fields, D. Rodriguez, K. N. Gary, E. C. Liebenberg, and J. C. Lotz, “Influence of Biochemical Composition on Endplate Cartilage Tensile Properties in the Human Lumbar Spine,” *J Orthop Res*, vol. 32, no. 2, pp. 245–252, Feb. 2014, doi: 10.1002/jor.22516.

[112] G. A. Whitney *et al.*, "Thyroxine Increases Collagen Type II Expression and Accumulation in Scaffold-Free Tissue-Engineered Articular Cartilage," *Tissue Eng Part A*, vol. 24, no. 5–6, pp. 369–381, Mar. 2018, doi: 10.1089/ten.tea.2016.0533.

[113] J. DeGroot *et al.*, "Accumulation of advanced glycation endproducts reduces chondrocyte-mediated extracellular matrix turnover in human articular cartilage," *Osteoarthritis and Cartilage*, vol. 9, no. 8, pp. 720–726, Nov. 2001, doi: 10.1053/joca.2001.0469.

[114] M. M. C. Steenvoorden *et al.*, "Activation of receptor for advanced glycation end products in osteoarthritis leads to increased stimulation of chondrocytes and synoviocytes," *Arthritis & Rheumatism*, vol. 54, no. 1, pp. 253–263, 2006, doi: 10.1002/art.21523.

[115] J. A. Martin *et al.*, "Mitochondrial electron transport and glycolysis are coupled in articular cartilage," *Osteoarthritis and Cartilage*, vol. 20, no. 4, pp. 323–329, Apr. 2012, doi: 10.1016/j.joca.2012.01.003.

[116] K. Johnson *et al.*, "Mediation of spontaneous knee osteoarthritis by progressive chondrocyte ATP depletion in Hartley guinea pigs," *Arthritis Rheum*, vol. 50, no. 4, pp. 1216–1225, Apr. 2004, doi: 10.1002/art.20149.

[117] J.-P. St-Pierre, Q. Wang, S. Q. Li, R. M. Pilliar, and R. A. Kandel, "Inorganic Polyphosphate Stimulates Cartilage Tissue Formation," *Tissue Engineering Part A*, vol. 18, no. 11–12, pp. 1282–1292, Jun. 2012, doi: 10.1089/ten.tea.2011.0356.

[118] W. D. Lee, R. Gawri, T. Shiba, A.-R. Ji, W. L. Stanford, and R. A. Kandel, "Simple Silica Column–Based Method to Quantify Inorganic Polyphosphates in Cartilage and Other Tissues," *Cartilage*, vol. 9, no. 4, pp. 417–427, Oct. 2018, doi: 10.1177/1947603517690856.

APPENDIX I – POLYP ASSAY VALIDATION

The protocol developed by Lee et al. [118] includes spiking half the samples with a known amount of polyP (7 nmol) to calculate the recovery ratio and to adjust for polyP lost in the column. Initial attempts at the assay were giving repeatedly low recovery rates, particularly for the LG-HV condition. Therefore, we wanted to validate the methods and identify at which part of the process we could potentially be losing polyP causing low recovery rates. We initially tested whether the presence of proteinase K could be digesting polyP or if the polymer could be hydrolyzed during the incubation period (Figure A1.1). No major differences in the polyP levels are observed and suggests that this stage is not the cause of low polyP recovery rates.

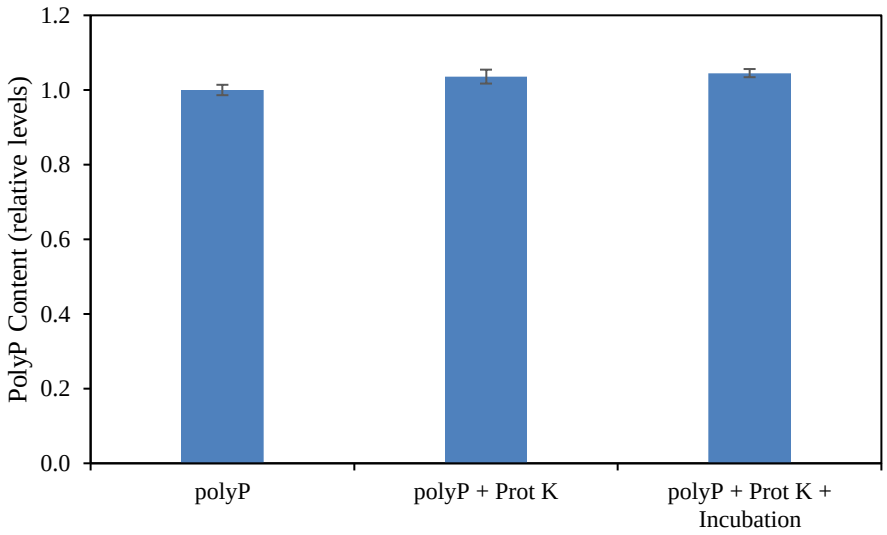

Figure A1.1 Relative levels of polyP, polyP with proteinase K, and polyP with proteinase K and incubation. Data is represented as mean ± SD.

Next, we investigated levels of polyP before and after processing through the column (Figure A1.2). Here, we noticed a 25% decrease in polyP content after the column. We also tested whether the nucleases were digesting polyP in the final step in the protocol, yet no major loss in polyP was reported (Figure A1.3). The LG-HV condition has particularly high levels of sGAG in

the tissue which can also bind to the column and lead us to speculate that saturation of the column was preventing polyP from binding. To address this, we increased the volume of proteinase K to 30 µL/mg wet weight to increase matrix digestion and release more polyP as well as dilute GAG and DNA which are potentially blocking sites available for polyP. We also switched the vendor of silica column used from EconoSpin to Qiagen since the latter option have a greater binding capacity. Despite making these adjustments, polyP quantification in tissues reported a negative recovery rate for the LG-HV condition which suggests that there was more polyP in unspiked samples than spiked samples. This may be explained by polyP being lost through the column, particularly in the spiked samples. PolyP has been reported to bind to proteins and could potentially bind to proteinase K and pass through the column. Also, precipitation may be preventing polyP from binding to the column.

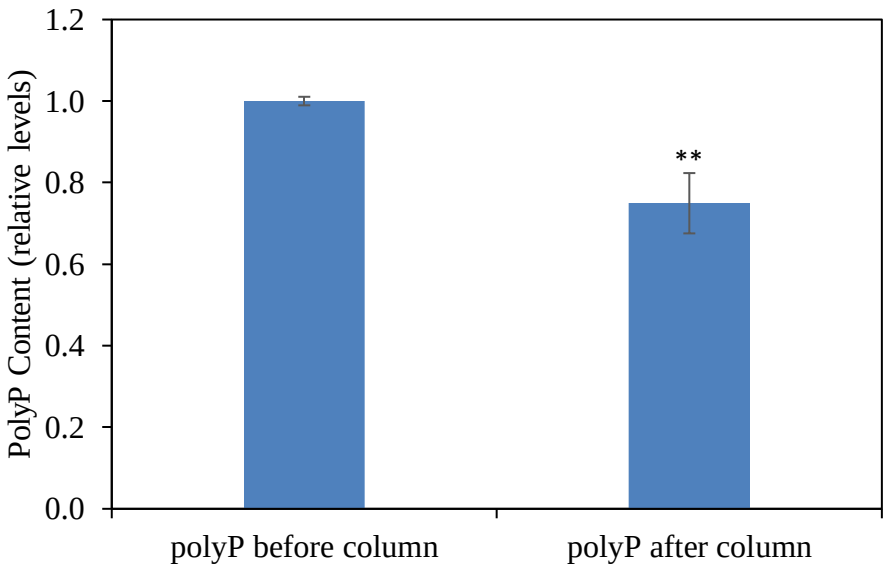

Figure A1.2 Relative polyP content before and after processing through the spin column. Data are represented as mean ± SD. Statistically significant decrease in polyP content compared to before the spin column is denoted by **($p<0.01$).

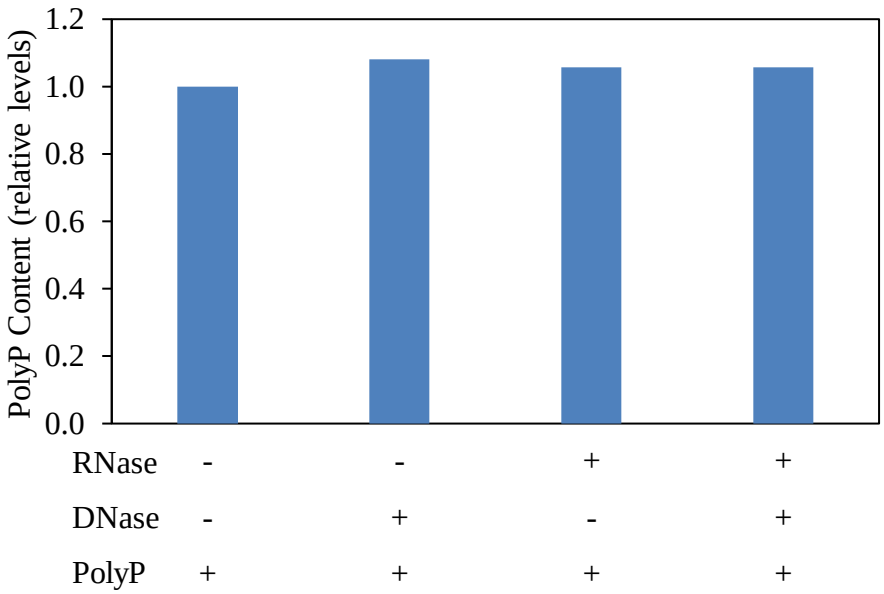

Figure A1.3 Relative polyP levels with (+) or without (-) RNase, DNase, and polyP. Data obtained from one replicate.

For this thesis we have decided to report the unspiked values of polyP in the tissues without accounting for the amount that was lost through the column using the recovery rates. Even without adjusting the polyP content, the LG-HV often has the highest polyP content in each set, yet the lowest recovery rate. This suggests that the polyP content in the LG-HV condition would have even greater reported polyP values if we did account for the recovery rates. These results are at odds with Lee et al who reported that greater polyP content has higher recovery ratios.

Future tests should consider starting the extraction process by bursting the cells in water without proteinase K. Subsequently, the samples could be incubated with chondroitinase ABC to digest GAGs and nucleases to digest DNA and RNA that may be binding to the column as well as phosphatase inhibitors to prevent digestion of polyP. Following this initial incubation period, proteinase K could then be added to digest remaining proteins in the matrix. In theory, this method would digest all biological molecules that can potentially bind to the column except for polyP.